Gold Nanoparticle-Based Colorimetric Sensing of Metal Toxins

12

Nivedita Priyadarshni and Nripen Chanda

Abstract

Miniaturized sensing devices have emerged as prevailing micro-scale analysis devices in the past few decades. In this context, metal nanoparticle-based sensors have proved their potential in developing highly sensitive and selective on-site detection techniques for various analytes and environmental toxins. Among various environmental pollutants, heavy metal contamination is the most severe problem worldwide because of its potential toxicity and non-biodegradable nature, even at lower exposure levels. Conventional analytical techniques for measuring metal toxins include atomic absorption spectroscopy (AAS), inductively coupled plasma mass spectroscopy (ICP-MS), and reversed-phase high-performance liquid chromatography. These methods give accurate results but are time-consuming, require a dedicated laboratory setup, sophisticated equipment setup, and trained personnel to operate. Therefore, an alternative user-friendly and cost-effective method is required for rapid and real-time monitoring of heavy metal toxins in groundwater and industrial wastewater monitoring. Efforts are being made in developing metal nanoparticle-enabled sensors because of distinct optical and electrical properties, which renders better selectivity, sensitivity, and portability that can be readily used in developing commercial products. The sensing process is based on the aggregation of nanoparticles in the presence of specific metal ions coupled with visible color change detected by naked eyes, indicating the presence of targeted heavy metal toxins. This chapter summarizes

N. Priyadarshni · N. Chanda (✉)
Material Processing and Microsystem Laboratory, CSIR-Central Mechanical Engineering Research Institute, Durgapur, West Bengal, India

Academy of Scientific and Innovative Research (AcSIR), Ghaziabad, Uttar Pradesh, India
e-mail: n_chanda@cmeri.res.in

273

various synthesis processes and potential colorimetric-based sensing applications of metal nanoparticle-enabled sensors for assessing clean and safe drinking water.

Keywords

Metal nanoparticles · Gold nanoparticles · Metal toxins · Colorimetric sensing · Lab-on-phone · Machine learning

Abbreviations

AAS	Atomic adsorption spectroscopy
AgNP	Silver nanoparticle
AHMT	Amino-3-hydrazino-5-mercapto-1,2,4-triazole
AI	Artificial intelligence
ANN	Artificial neural network
CE	Counter electrode
CNN	Convolutional neural network
CTAB	Cetyl-trimethyl ammonium bromide
DLVO	Derjaguin–Landau–Verwey–Overbeck
DMSA	Dimercaptosuccinic acid
DTPA	Diethylenetriaminepentaacetic acid
EDL	Electric double layer
EPA	Environmental Protection Agency
GNP	Gold nanoparticles
GNR	Gold nanorod
GSH	Glutathione
HPLC	High-performance liquid chromatography
ICP-MS	Inductively coupled plasma mass spectrometry
LOC	Lab-on-chip
MBA	Mercaptobenzoic acid
ML	Machine learning
MLR	Multiple linear regression
MNP	Metal nanoparticles
NADH	Nicotinamide adenine dinucleotide hydrogen
PCD	Paper-based colorimetric device
PEG	Polyethyleneglycol
PPB	Parts per billion
PtNP	Platinum nanoparticle
PVA	Polyvinyl alcohol
PVP	Polyvinylpyrrolidone
RE	Reference electrode
RGB	Red, green, blue
SPR	Surface plasmon resonance
SVM	Support vector machine

TA	Thioctic acid
TDA	Thiodiacetic
TG	Thioguanine
TMB	Tetramethylbenzidine
TOAB	Tetraoctylammonium bromide
WE	Working electrode
WHO	World Health Organization
XRF	X-ray fluorimetry

12.1 Introduction

Metals are always considered important materials in manufacturing, science, engineering and technology, and commercial aspects (Santos 2017). These bulk metals, when fragmented to nanosize having dimensions 1–100 nm, are termed metal nanoparticles or metallic nanoparticles (MNP) (Venkatesh 2018). The advent of MNP marked a revolutionary change in sensing technology and biology because of distinct electronic, optical, biochemical, and physicochemical properties. Facile synthesis and surface modification of MNPs with diverse functional moieties like antibodies, enzymes, ligands, proteins, and drugs of interest facilitate target-oriented binding with analytes rendering selectivity and an efficient sensing platform. The large surface-area-to-volume ratio and spatial confinement of free electrons offer massive numbers of binding sites on the surface of metal nanoparticles (MNP). It brings an excellent scaffold to immobilize with large quantities of ligands and biomolecules, making it highly interactive with the analytes (Venkatesh 2018; Siontorou 2019). Metal nanoparticles (like gold, silver, copper, and platinum nanoparticles) have the exceptional feature of absorption and scattering of light that originates from the collective oscillation of surface electrons to unique optical properties of MNPs (Vasquez et al. 2018; Maghsoudi et al. 2021). When exposed to appropriate frequencies of electromagnetic waves (light), it induces the excitation of electrons on the surface of MNPs known as surface plasmon resonance (SPR). This property of MNPs is also responsible for their vibrant color in an aqueous solution and can be easily tuned by changing the shape and size of the metal nanoparticle. For example, gold nanospheres of ~20 nm diameters appear wine red in color. However, their color becomes purple and blue as the size increases to ~100 nm. Likewise, the silver nanoparticle of 20 nm is yellow colored in an aqueous solution, and with the increasing size of the silver nanoparticle, color changes to red (Shrivas et al. 2015; Venkatesh 2018; Willner and Vikesland 2018). This size-dependent change in color of metal nanoparticles can be exploited to develop visual colorimetric sensors (chemical sensors, biosensors, and electro-optical sensors) where small nanoparticles aggregates in the presence of analytes change in color of the solution (Chen et al. 2014b). The metal nanoparticles are synthesized by two approaches, top-down and bottom-up (Wang and Xia 2004). Top-down synthesis involves bulk

material as a precursor, broken down to nano-range particles using different physical lithography techniques such as soft lithography and electron-beam lithography. Top-down plays a vital role in the large-scale fabrication of nanostructure; it has limitations such as imperfections in resulting material, expensive, and time-consuming (Khandel et al. 2018). Bottom-up synthesis relies on the assembly of molecules or atoms to build complex nano-constructs. Some common processes used in bottom-up methods include sol-gel (Epifani et al. 2000), chemical vapor deposition (Murty et al. 2013), laser ablation (Kumari et al. 2014), and solvo-thermal method (Choi et al. 2013), but the most popular is the chemical reduction that provides the advantage of fine control over shape and size of the nanoparticle. The chemical reduction method of nano-metal synthesis involves reducing precursor metal salt in the presence of a suitable stabilizer. The quasi-spherical-shaped nanoparticles are thermodynamically most stable; therefore, the synthesis of spherical nanoparticles with different size ranges can be easily achieved by altering the concentration of precursor salt, concentration and rate of addition of reductant, and temperature. Since the optical properties of nanostructures vary with shape and size, a process to synthesize non-spherical nanoparticles has been developed to utilize these anisotropic nanostructures in different applications. Anisotropic metal nanostructures are synthesized by step-wise growth in the presence of nanoparticle seed and structure-directing agents, like cetyl-trimethyl ammonium bromide (CTAB) (Murphy et al. 2011; Chang and Murphy 2018). High surface energy and short inter-particle distances of nanoparticles make them unstable and coalesce, forming thermodynamically favored stable bulk particles. In the absence of interfering repulsive forces, metal nanoparticles attract each other resulting in larger aggregates. To maintain spatial confinement in the nano range, stabilization of metal nanoparticles is essential, which can be accomplished by steric or electrostatic stabilization using stabilizing agents like polymer, ligands, and surfactants having suitable functional groups (Olenin 2019; Sperling and Parak 2010). Stabilization of metal nanoparticles leads to the formation of an electric double layer that furnishes repulsive force to remain without aggregated in dispersed form (Venkatesh 2018; Polte 2015). Functionalization of metal nanostructures with proper capping agents not only provides stability to nanoparticles but also renders specificity toward target analytes and, thus, finds several applications in sensing (Yu and Li 2019), drug delivery (Ghosh et al. 2008), cell imaging, and photothermal therapeutics (McQuaid et al. 2016).

In the present rapid industrialization scenario, heavy metal contamination in the environment is a significant problem globally. The presence of excessive levels of heavy metal pollutants in soil and water affects the quality of surface and groundwater, resulting in a severe threat to human health and the deterioration of environmental resources. The heavy metal pollutant enters water bodies by various natural and anthropogenic sources, including mining, manufacturing, industrial, and municipal waste discharge (Poornima et al. 2016). Arsenic, chromium, lead, mercury, and cadmium are some of the most concerning heavy metals due to their high toxicity, even at low concentrations. Therefore, regulatory organizations like Environmental Protection Agency (EPA) and World Health Organization (WHO) set a standard on
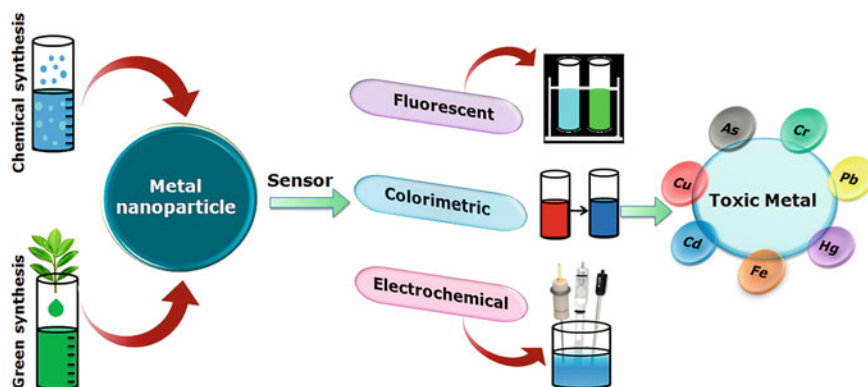
Fig. 12.1 General schematic of MNP synthesis and their use in sensing applications of toxic metal ions

permissible limits of heavy metal consumption (Varun and Kiruba Daniel 2018; Zhang et al. 2019a; Li et al. 2013; Tchounwou et al. 2012). Consumption of heavy metals above permissible limit triggers bio-toxic effects by altering cellular activities and developing severe disorders, including cancer. Since they are not quickly metabolized or excreted, they tend to accumulate in soft tissues for years, which slowly causes mental and central nervous dis-functioning, damage to the liver, kidneys, lungs, and other vital organs (Li et al. 2013). The traditional techniques for detecting these toxic metals are based on either spectroscopy or chromatography, which includes inductively coupled plasma mass spectrometry (ICP-MS), atomic adsorption spectroscopy (AAS), inductively coupled plasma optical emission-spectrometry (ICP-OES), X-ray fluorescence spectrometry (XRF), and high-performance liquid chromatography (HPLC). These techniques are highly selective, sensitive, and efficient in quantification; their large-scale implementation is still a challenge due to their complexity and sophisticated installation procedure. More-over, they require technical expertise to operate, involve toxic chemicals, multiple sample preparation steps, time-consuming, and dedicated laboratory setup, and time-to-time maintenance of instruments makes analysis highly expensive (Zhang et al. 2019a; Lu et al. 2018; Buledi et al. 2020). Thus, there is a need to develop an inexpensive heavy metal detection technology that is rapid, easy-to-handle, user-friendly, portable, and operated as a point-of-use device. In this context, nanoparticle-enabled colorimetric sensing technology has huge potential to detect metal toxins on-site with improved performance as a device in terms of selectivity, sensitivity, and reproducibility that can be readily developed into commercial products. A general schematic of MNP synthesis and its advantages in sensing application has been shown in Fig. 12.1. This chapter reviews the colorimetric sensing strategies for heavy metals based on aggregation and dispersion of metal nanostructure, specially focusing on gold nanoparticle-based sensors. It also highlights recent advances in developing a miniaturized, point-of-use colorimetric sensor for metal toxins on paper substrate. Moreover, the integration of smartphone

camera readouts and machine learning approach with colorimetric sensors introduces a new lab-on-mobile concept, which has been discussed in the later section of this chapter.

12.2   Metal Nanoparticle-Based Sensor

Sensors are devices that convert the chemical or physical properties of a specific analyte into a measurable signal proportional to the analyte concentration (Jayabal et al. 2015a). Metal nanoparticle-based sensing devices are characterized in three units, i.e. (a) metal nanoparticle, (b) a recognition component that furnishes selectivity, and (c) a signal transduction system, which supplies information about the presence and absence of analyte (metal toxin) in a sample (Willner and Vikesland 2018; Mahato et al. 2018). The resultant signals originating from the MNP sensor can be of different types, and based on these signals, sensors can be categorized as optical, electrochemical, and piezoelectric sensors (Willner and Vikesland 2018). Optical sensor depends on the interaction of toxic metals with electromagnetic radiation (like ultraviolet, visible, or infrared light) in the form of emission or absorption, which spectroscopic techniques can monitor. Colorimetric and fluorescence are two methods commonly used as reporting signals in optical sensors. Colorimetric sensing is based on surface plasmon resonance of metal nanoparticles. SPR peak of the metal nanoparticle is highly sensitive to the inter-particle distance between nanoparticles. Plasmon coupling causes aggregation of metal nanoparticles with pronounced color change and concomitant red-shift of SPR peak. Most of the gold/silver nanoparticle-based colorimetric sensors explore the property of color change coupled with aggregation and dispersion of nanoparticles in the presence of target heavy metal (Doria et al. 2012). The fluorescence sensor consists of a fluorophore as a signal-transducing element, which exhibits the property of photoluminescence. When the fluorophore is irradiated with electromagnetic radiation, it absorbs the photon energy, and its orbital electrons are excited to a higher energy level (singlet state). Fluorescence occurs when the excited electron relaxes to a lower energy state (ground state) by emitting a photon. Upon interaction with the heavy metal toxin, the fluorescent signal changes as either "turn-off" or "turn-on." The metal nanoparticles of size 3 nm or smaller (like nanodots and nanoclusters) can be directly used as a fluorescent marker as they exhibit inherent fluorescence properties. Moreover, MNPs which lack their fluorescence can be functionalized with a fluorophore to obtain a fluorescent sensor. Quenching and restoration of fluorescence property indicate interaction of toxic metal and nanoparticle-based changes in the sensor (Xiong et al. 2019; Willner and Vikesland 2018). An electrochemical sensor is a device that transforms chemical reactions into electrical signals (Alam et al. 2020). When an electrical circuit is introduced to heavy metal, the molecular binding of toxic metal near electrode surface initiates oxidation/reduction process, which generates or modulates electrical current in the form of charge (electron) transfer between the electrode and toxic metal ion. This charge transfer may lead to the completion of an incomplete circuit or alteration in current, potential,

or resistance measured by instruments like potentiostat or galvanostat (Willner and Vikesland 2018; Doria et al. 2012). Electrochemical sensors may exist in a two-electrode system or three-electrode system (Andrea Scozzari 2008). In the two-electrode arrangement, a working electrode (WE) is coupled with a counter electrode (Auxiliary, CE), and the difference of electric potential is measured between WE and the potential of CE. Examples of the two-electrode system are amperometric sensor (measures electric current between CE and WE in the presence of a constant electric potential) (Sahin and Kaya 2019) and potentiometric sensor (measures the potential difference between two electrodes, i.e., WE and CE in the absence of current flow) (Isildak and Özbek 2020). Three-electrode consists of a reference electrode (RE) along with WE and CE. The best example for a three-electrode system is a voltammetric sensor, which measures current response as a function of applied potential. Current is linearly dependent on the concentration of electro-active species (toxic metal ion) (Power and Morrin 2013). Among these sensors, colorimetric sensors have several advantages: simplicity, unmatched sensitivity, and inexpensive and fast detection time. Moreover, it operates in a visible range of the electromagnetic spectrum. The resultant signals can be detected by naked eyes, making it possible for wide-scale use by the common people. Therefore, it gained huge attention for quick detection of metal toxins in solutions (Kim et al. 2012; Jayabal et al. 2015b).

12.3   MNP-Based Colorimetric Detection Strategies

Metal nanoparticles are highly flexible because of precise control on size, shape, composition, assembly, and optical properties during the synthetic process. Thus, it has been extensively investigated for colorimetric sensing of toxic metal ions. WHO has standardized the consumption limit for these toxic metal ions; for instance, the permissible limit for arsenic is 10 ppb, chromium 50 ppb, lead 15 ppb, mercury 2 ppb, copper 15 ppb, and cadmium 5 ppb. Thus, their trace level monitoring is essential, and for which researchers are coming up with new techniques based on metal nanoparticles. This section deals with MNPs-based colorimetric sensors for the determination of toxic metals. Zhou et al. reported 4-mercaptobenzoic acid (4-MBA) modified silver nanoparticles (AgNP) for colorimetric sensing of Cu^{II} ion in water. 4-MBA consists of –SH group that binds with AgNP and –COOH groups exposed on the surface that chelates Cu^{II} forming carboxylate–Cu^{II}–carboxylate bridges. Chelation of Cu^{II} causes aggregation of AgNP and color changes from yellow to purple (Fig. 12.2a) (Zhou et al. 2011). Chen and coworkers demonstrated a paper-based colorimetric device (PCD) for Hg^{II} detection using citrate stabilized PtNP. 3,3,5,5-tetramethylbenzidine (TMB) and H_2O_2 produce blue color in the presence of PtNP that mimics the peroxidase activity by catalyzing the reaction. However, the introduction of Hg^{II} in the reaction system inhibits the catalytic activity of PtNP resulting in a color change from blue to colorless. (Fig. 12.2b) (Chen et al. 2016). Shrivas et al. reported colorimetric sensing of Pb^{II} using polyvinyl alcohol (PVA) functionalized AgNP and paper-based analytical devices.
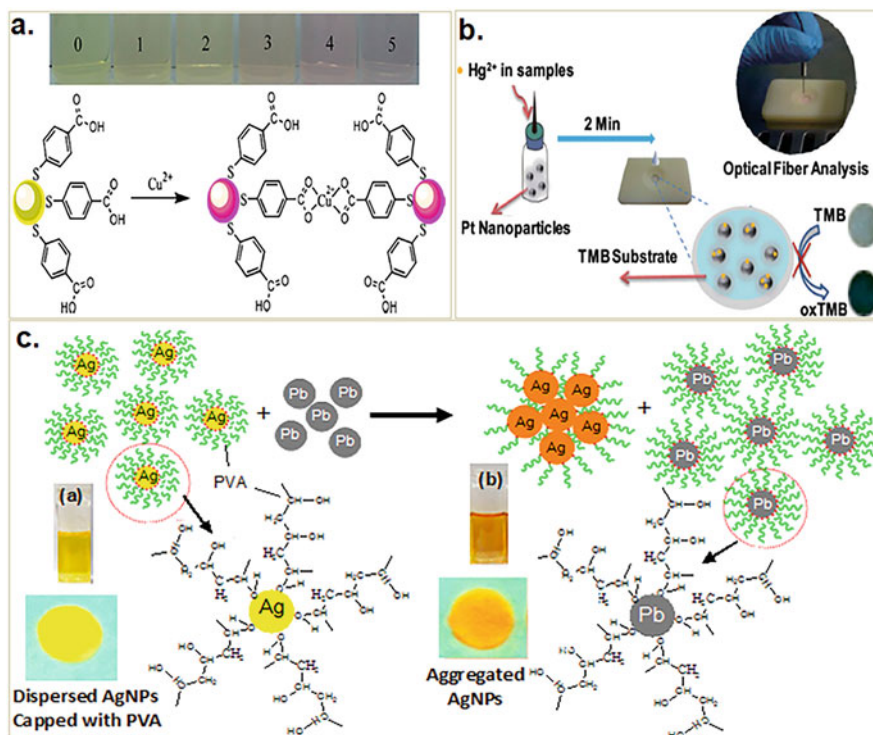
Fig. 12.2 Metal nanoparticle-based colorimetric sensor for heavy metal. (**a**) 4-MBA-AgNP-based colorimetric detection of Cu^{II} with color change from yellow to purple. (**b**) Paper-based analytical device for detection of Hg^{II} using PtNP in the presence of TMB and H$_2$O$_2$. (**c**) Colorimetric sensing of Pb^{II} using PVA-AgNP coated paper substrate showing color change from yellow to red. Reproduced from Ref. Zhou et al. (2011) (**a**). Open access with proper citation (**b**). Reproduced from Ref. Shrivas et al. (2019) (**c**)

After interaction of Pb^{II} with AgNP-PVA, the color changes from yellow to red and color intensity were recorded on a smartphone followed by processing in ImageJ software (Fig. 12.2c) (Shrivas et al. 2019). Similar color-based sensing methods have been reported for toxic metals like As^{III}, Cr$^{III/VI}$, Cd^{II}, Pb^{II}, Cu^{II}, and Hg^{II} using modified metal nanoparticles including Au, Ag, Pt, and Pd nanoparticles, which have been listed in Table 12.1. Silver and gold nanoparticles exhibit prominent SPR-based properties associated with a color and have been widely explored for the same. Though Pt-like nanoparticles exhibit SPR features, they are examined mainly for their catalytic activity and enzyme mimetic behavior for inducing an indirect color change in sensor application. Among all these metallic nanoparticles, gold nanoparticles (GNP) received much attention in colorimetric sensing applications (Singla et al. 2016). GNP can be prepared by simple methods with high stability and provides a suitable platform for multi-functionalization with various biological and organic ligands for selective binding of target toxins. They have a high surface-to-

Table 12.1 MNP-based colorimetric sensing of toxic metal in solution and paper-based analytical devices

MNP	Synthesis process	Modification	Target metal	LOD (ppb)	Dynamic range (ppb)	Method of detection	Ref
AgNP	Chemical reduction by NaBH$_4$ in presence of polyvinylpyrrolidone (PVP)	Aptamer	As^{III}	6 0.0	50–700	Aggregation	Divsar et al. (2015)_
	Chemical reduction by trisodium citrate	Polyethyleneglycol (PEG)	As^{III}	1.0	1.0–15	Yellow→blue (aggregation)	Boruah et al. (2019)
	Chemical reduction by NaBH$_4$	Trisodium citrate	Cr^{VI}	0.075	0.05–5 × 10^4	Yellow→purple (aggregation)	(Ravindran et al. 2012)
	Chemical reduction by NaBH$_4$	Tartrate	Cr^{III}	3.1	5.19–60.7	Yellow→red (aggregation)	Xu et al. (2013)
	NaOH	3,4-dihydroxyphenylalanine (L-dopa)	Cr^{VI}	10	10–1 × 10^4	Yellow→brown (aggregation)	(Joshi et al. 2016)
	Chemical reduction by NaBH$_4$	Tartrate	Cr^{III} Cr^{VI}	2.0 3 0.0	5 – 100 10 – 100	Yellow→red (aggregation)	Shrivas et al. (2016)
	Green synthesis by fruit extract of *Durantaerecta*	Phytochemicals	Cr^{VI}	100	1 × 10^4– 1 × 10^5	Yellow→colorless (aggregation)	Ismail et al. (2018)
	Chemical reduction by NaBH$_4$	Polyvinylpyrolidone (PVP)	Cr^{VI}	1.7	5.19–124.5	Yellow→red (aggregation)	He et al. (2019)
	Chemical reduction by NaBH$_4$	Trisodium citrate	Cr^{VI}	26	10–700	Point-of-care device; yellow→red	Kumar et al. (2020)
	Green synthesis using L-tyrosine reduction	L-tyrosine	Hg^{II}, Mn^{II}	0.8	3.2–132	Yellow→colorless (etching of AgNP) Yellow→brown (aggregation)	Annadhasan et al. (2014)
	Green synthesis by fruit extract of water apple (*Syzygium aqueum*)	Phytochemicals	Hg^{II}	170	1002–20,050	Yellow→colorless (aggregation)	Firdaus et al. (2017)

(continued)

Table 12.1 (continued)

MNP	Synthesis process	Modification	Target metal	LOD (ppb)	Dynamic range (ppb)	Method of detection	Ref
	Green synthesis (leaf extract)	2-aminopyrimidine-4,6-diol	Hg^{II}	0.35	0–13,033	Brown→yellow (aggregation)	Prasad et al. (2018)
	Chemical reduction by $NaBH_4$ in the presence of polyvinylpyrolidone (PVP)	Methionine	Hg^{II}	0.2	4–20	Yellow→colorless (aggregation)	Balasurya et al. (2020)
	Chemical reduction by $NaBH_4$	Polyvinyl alcohol (PVA)	Pb^{II}	20	50–1000	Paper-based analytical device (yellow→red)	Shrivas et al. (2019)
	Green synthesis by 3,4-dihydroxy-l-phenylalanine (DOPA) in the presence of NaOH	DOPA (mussel-inspired protein)	Pb^{II} Cu^{II}	0.019 0.005	0.012–31	Yellow→red Yellow→brown	Cheon and Park (2016)
	Chemical reduction by dopamine in the presence of NaOH	Dopamine	Cu^{II}	3.2	3.2–512	Yellow→brown	Ma et al. (2011)
	Chemical reduction by $NaBH_4$	4-mercaptobenzoic acid	Cu^{II}	1.5	6.35–6350	Yellow→purple	Zhou et al. (2011)
	Chemical reduction by $NaBH_4$	Gelatin hydrogels	Cu^{II}	0.63	0.63–6350	Yellow→green	Jeevika and Ravi Shankaran (2014)
	Chemical reduction by $NaBH_4$ in the presence of KOH and ethanol	N-acetyl-L-cysteine	Fe^{III}	4.4	4.4–4464	Brown→colorless	Gao et al. (2015)
	Chemical reduction by $NaBH_4$	5-sulfosalicylic acid	Cd^{II}	0.33	0–123.6	Yellow→red	Jin et al. (2015)
	Chemical reduction by trisodium citrate	1-amino-2-naphthol-4-sulfonic acid	Cd^{II}	9.7	0–1124	Yellow→brown	Huang et al. (2016)

NP	Synthesis method	Capping agent	Metal	LOD	Range	Mechanism/Color change	Reference
Pt NP	Chemical reduction by NaBH$_4$ in the presence of trisodium citrate	Trisodium citrate	Ag^{I}	8.4×10^{-4}	0.001–0.32	Blue→colorless (peroxidase mimetic activity of PtNP inhibited by Ag^{I})	Wang et al. (2017)
	Chemical reduction by trisodium citrate	Trisodium citrate	Hg^{II}	16.04	–	Blue→colorless (peroxidase mimetic activity of PtNP inhibited by Hg^{II})	Bertolacci et al. (2020)
	Chemical reduction by NaBH$_4$	Trisodium citrate	Hg^{II}	2.0	0–20,050	Paper-based colorimetric Device (PCD) (blue→colorless Peroxidase mimetic activity of PtNP inhibited by Hg^{II})	Chen et al. (2016)
Pt-se NP	Chemical reduction by ascorbic acid	Polyvinylpyrolidone (PVP)	Hg^{II}	14.0	0–501	Blue→colorless (peroxidase mimetic activity of PtNP inhibited by Hg^{II})	Guo et al. (2017)
Ag-Cu	Chemical reduction by NaBH$_4$	Trisodium citrate	Hg^{II}	0.1	0.2–2.0	Yellow→light orange	Li et al. (2018b)
Au-Ag	Trisodium citrate	Poly(diallyl dimethylammonium chloride)	Hg^{II}	1	0.5–80	Brownish–orange→purple	Mathaweesansum et al. (2020)
Au-Ag	Chemical reduction by NaBH$_4$	Chitosan	Hg^{II}	0.18	0.18–18,045	Brown→purple	Zhang et al. (2019b)
Au-Ag	Chemical reduction by NaBH$_4$	Trisodium citrate	Pb^{II}	5.28	2–20	Reddish orange→purple	Sahu et al. (2020)

volume ratio and exhibit unique optoelectrical and catalytic properties imparting useful surface plasmon behavior that generates a detectable response in the presence of metal ions. These distinctive properties make them "star" among the other nanoparticles providing researchers a broad spectrum for sensor application (Jans and Huo 2012).

12.4 Synthesis, Functionalization, Properties, and Sensing Strategy of GNP

12.4.1 Synthesis of GNP

The sensing application of gold nanostructures is dependent mainly on their shape, size, and surface functionality, and thus selection of suitable synthetic procedures is crucial in designing a sensor (Yeh et al. 2012; Yu and Li 2019). In the last few decades, numerous chemical and physical procedures are adopted to precisely control the shape, size, and mono-dispersity of nanoscale gold. However, green synthesis technologies involving biological entities are gaining much attention nowadays due to the environmental-friendly and biologically safe approach to synthesizing gold nanoparticles (Zhang et al. 2020). The details of some commonly used synthesis procedures for nanoscale gold are summarized here.

12.4.1.1 Turkevich–Frens Method

Turkevich first reported the synthesis of gold nanoparticles in 1951 (Turkevich et al. 1951). In this method, gold chloride salt ($HAuCl_4$) is heated (~90 °C) in the presence of a reducing agent like sodium citrate resulting in monodispersed spherical gold nanoparticle suspended in the water of around 20–40 nM in diameter (Fig. 12.3a). Here, citrate plays the role of both stabilizing and reducing agents (Saha et al. 2012). Later, in 1973, Frens improved this protocol and prepared gold nanoparticles of different sizes ranging between 16 and 147 nm. This method provides precise control over the size of the gold nanoparticle by adjusting the proportion of chloroauric acid salt to sodium citrate solution (Razzaque et al. 2016). The citrate reduction provides a negative surface charge to gold nanoparticles and prevents aggregation by imposing repulsion induced by Coulombic force (Chen et al. 2014a). Citrate forms a weak coordination layer with gold nanoparticles that adds easy replacement of citrate with functionalizing agents like thiols (Zhu et al. 2003), polymers, and biomolecules (Nghiem et al. 2010).

12.4.1.2 Brust–Schiffrin Method

In 1994, Brust and Schriffin introduced another protocol for synthesizing gold nanoparticles in an organic medium that results in water-immiscible gold nanoparticles (Brust et al. 1994). This synthetic strategy involves bi-phasic reduction of gold salt to produce thiol-protected gold nanoparticles (Li et al. 2011; Perala and Kumar 2013). The gold chloride salt is transferred from the aqueous phase to the organic phase (toluene) using the surfactant tetraoctylammonium bromide (TOAB)
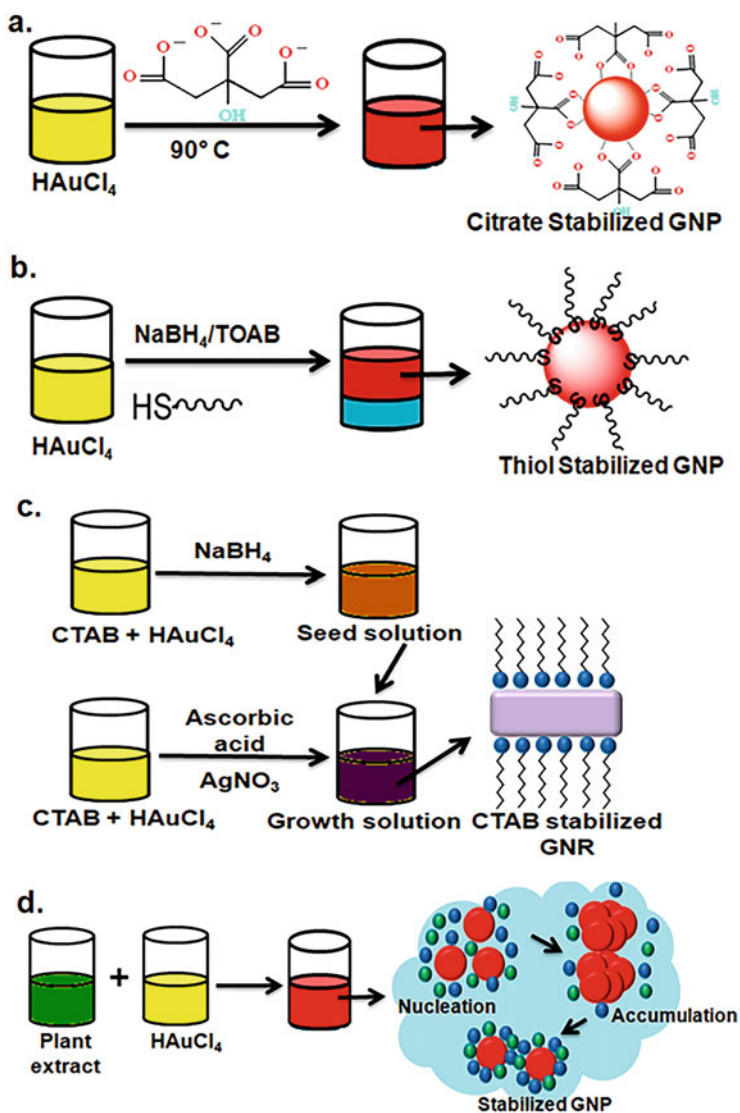
Fig. 12.3 Various synthesis procedures of gold nanoparticles. (**a**) Turkevich–Frens method. (**b**) Brust–Schiffrin method. (**c**) Seed-mediated growth method for anisotropic gold (GNR). (**d**) Green synthesis of GNP using plant extract

followed by the addition of dodecanethiol as a stabilizing agent. Next, sodium borohydride (a strong reducing agent) is added that reduces gold salt to thiol-stabilized gold nanoparticles producing deep brown color in toluene (Fig. 12.3b). This method results in 1.5–5 nm gold nanoparticles having low dispersity.

Alkanethiol forms a monolayer on GNP surface enabling easy modification with various functional groups (Saha et al. 2012).

12.4.1.3 Seed-Mediated Growth

The seed-mediated growth is the most reputed procedure used in the preparation of anisotropic gold nanoparticles like nanorod (GNR), introduced by Murphy and coworkers (Jana et al. 2001) and El-Sayed group (Nikoobakht and El-Sayed 2003). Cetyltrimethyl ammonium bromide (CTAB), a surface-active molecule, is used as the template for directed growth of anisotropic nanostructures (Meng et al. 2019). The synthesis of gold nanorod is achieved in two steps (Fig. 12.3c). Step 1 involves the seed solution synthesis where a golden brown–colored gold seed is prepared by reducing gold chloride salt ($HAuCl_4$) with freshly prepared ice-cold borohydride ($NaBH_4$) sodium in the presence of CTAB. Step 2 involves the growth of nanorods in the presence of CTAB and silver nitrate ($AgNO_3$). Gold salt is reduced with a mild reductant ascorbic acid followed by seed solution. The growth solution is left undisturbed for 12 hrs to grow the seed crystals into gold nanorod under the action of surfactant (CTAB). The nanorods of desired aspect ratio (length/width) are achieved by altering the concentration of gold chloride salt and seed (Murphy et al. 2011; Li et al. 2018a).

12.4.1.4 Green Synthesis of Gold Nanoparticles

Green synthesis of nanoparticles emerged as an attractive substitute for conventional chemical synthesis procedures. This method involves the use of unicellular and multicellular biological entities like plant extracts, bacteria, actinomycetes, fungus, yeast, and viruses. The biological entities act as a factory for nanoparticle synthesis that offers non-toxic, inexpensive, and environmental-friendly approaches both extra and intra-cellularly without using toxic chemicals during synthesis, thus also termed as "Green chemistry" (Fig. 12.3d) (Baranwal et al. 2016; Zhang et al. 2020; Salem and Fouda 2021; Sengani et al. 2017) Das and coworkers synthesized 20 nm spherical gold nanoparticles by using flower extracts from *Nyctanthes arbor-tristis* (night jasmine) (Das et al. 2011). Narayanan and Sakthivel used leaf extracts of *Coriandrum sativum* to synthesize gold nanoparticles of size 7–58 nm (Narayanan and Sakthivel 2008). Husseiny group reported the extracellular preparation of GNP using a bacterial strain Pseudomonas aeruginosa. The mechanism involves the transfer of an electron from nicotinamide adenine dinucleotide hydrogen (NADH)-dependent reductase enzyme resulting in the reduction of Au^{3+} to Au^0 and itself oxidized to NAD^+ (Husseiny et al. 2007). Synthesis of nanoparticles using plant extracts is comparatively easier, faster, and cost-effective than bacterial synthesis as it does not require complex and multiple-step processes like isolation, culturing, and maintenance of bacterial strain (Iravani 2011).

12.4.2 Colloidal Stability of Gold Nanoparticles and Functionalization for Sensor Application

Colloidal stability of gold nanostructure depends largely on the surface energy, surface composition, and the inter-particle behavior arising from the surface and intermolecular forces. Nanoparticles exhibit high surface energy and short inter-particle distance, which make them unstable and result in aggregation. The chemistry behind the aggregation of the nanoparticle is complicated due to the involvement of different kinds of forces like electrostatic repulsion, van der Waals, and magnetic forces (Rance et al. 2010). However, the van der Waals force of attraction dominates due to short inter-particle distance, which compels them to form aggregates. Therefore, to avoid the agglomeration of nanoparticles, repulsive force is introduced by adding a capping agent during the synthesis of nanoparticles. The capping agents bind on the surface of the nanoparticle, providing two types of stabilization, electrostatic and steric. In an aqueous environment, most of the nanoparticles carry some surface charge due to ionization of the surface group or adsorption of charged molecules or ions. To balance the surface charge, a cloud of opposite charges is created. This charged cloud consists of the inner stern layer and outer diffuse layer forming an electric double layer (EDL), creating an electrostatic repulsive force between particles. In the case of steric stabilization, a physical barrier is created by the adsorption of ligands on the particle surface that prevents particles from aggregation (Amina and Guo 2020; Moore et al. 2015). The stabilization of gold particles was described by DLVO (Derjaguin–Landau–Verwey–Overbeck) theory of balance between the repulsive (electrostatic interactions) and the attractive force (van der Waal). According to DLVO theory, the sum of electrostatic and van der Waals force between two nanoparticles represents the total force acting on the colloidal solution (Zhou et al. 2009; Aldewachi et al. 2018).

Due to the nanometer size, gold nanoparticles have a high surface to volume ratio making them extremely active, and therefore, surface capping is required to lower the surface energy and increase stability. Surface functionalization of gold nanoparticles also renders specificity for the target analyte during the sensing procedure. Therefore, surface modification of GNP accomplishes two objectives: (1) chemical stability and (2) target-specificity (Zhang 2013). Gold nanoparticles can be functionalized by thiol-containing ligands, biomolecules, and polymers using different strategies like covalent coupling (Au-S bonding), specific recognition (e.g., antibody-antigen, DNA, aptamer), and electrostatic interaction. Sulfur-containing molecules are highly effective functionalizing agents, since, Au-thiol bonds are strong, resulting in highly stable gold nanoparticles. Many thiol-containing compounds like thioctic acid, glutathione, thioguanine, cystamine, thiolated–diethylenetriaminepentaacetic acid (SH-DTPA), and thiolated–PEG (SH-PEG) are used to modify gold nanoparticles and implicate in sensing of toxic metal ions (Mahato et al. 2019). Chai and coworkers reported glutathione functionalized gold nanoparticle (GSH-GNP) for Pb^{II} detection based on aggregation and red to blue color change of GSH-GNP (Chai et al. 2010). Xue and group demonstrated 6-mercaptonicotinic acid and L-Cysteine co-functionalized GNP as Cd^{II} sensor

(Xue et al. 2011). Wang and coworkers reported 4-amino-3-hydrazino-5-mercapto-1,2,4-triazole (AHMT) functionalized gold nanoparticles for colorimetric Cd^{II} detection. AHMT consists of thio, amino, and triazole groups which can form bonding with GNP surface. However, among these groups, thiol preferentially binds with GNP forming (Au–S) bond while other groups are involved in the chelation of Cd^{II} ion (Wang et al. 2013). Compared to other molecules, thiol-ligands bind easily with the gold nanoparticle surface, which can be attributed to the mechanism of ligand exchange that replaces the already bound ligand with the thiol compound without altering the structural integrity of GNP. Liu and Lu fabricated a lead biosensor using DNAzyme-directed aggregation of DNA modified gold nanoparticles. DNAzyme consists of an enzyme specific to Pb^{II} ions. DNA functionalized GNP forms a blue-colored assembly in the presence of DNAzyme. The introduction of Pb^{II} in reaction activates DNAzyme to cleave DNA stand and change the color of GNP from blue to red (Liu and Lu 2003). Lee and Mirkin developed a highly selective Hg^{II} detection assay based on thymine-Hg-thymine base paring. The GNP surface was functionalized with a thiol modified DNA probe (probe 1 and probe 2). Though the thiol modified-GNP is stable, it loses stability in the presence of Hg^{II}, forming a bridge of thymine-Hg-thymine, leading to mismatch in T–T base pairs. This causes red-colored GNP to turn blue leading to aggregation (Lee and Mirkin 2008).

12.4.3 Optical Properties

The refinement of bulk gold to nanoscale dimension allows them to interact with light, causing strong absorption at specific wavelengths. When gold nanoparticles are exposed to light, the electromagnetic field of light causes polarization of free electrons present on GNP's surface, resulting in their collective oscillation. When the frequency of incident light coincides with the frequency of collective oscillation of surface electrons, it absorbs the radiation of that particular wavelength giving an absorption band known as surface plasmon resonance (SPR). The SPR of gold nanostructures ranges from the visible to the near-infrared region of the electromagnetic spectrum depending on the size and shape of the gold nanoparticles (Fig. 12.4a) (Wang and Yu 2013). A spherical gold nanoparticle of 20 nm possesses SPR peak at 520 nm in the visible region responsible for the red color of the colloidal solution. As the size of the GNP increases, the SPR band gradually shifts to a higher wavelength with a concomitant color change of colloidal solution. Thus, the colored appearance (red, orange, brown, purple, and blue) of the colloidal gold solution is dependent on the size of gold nanoparticles (Amina and Guo 2020). Moreover, as the symmetry changes from spherical to nanorod, the SPR splits into two Plasmon bands known as transverse bands arising due to electron oscillation along the short axis (width) and longitudinal band due to electron oscillation along the long axis (length) (Fig. 12.4a) (Yasun et al. 2013). Richard Gans, in 1912, explained that the change in the shape of nanoparticles leads to alteration in position and number of SPR band and thus depends on the aspect ratio (length/width) of nanoparticles, not absolute dimension.
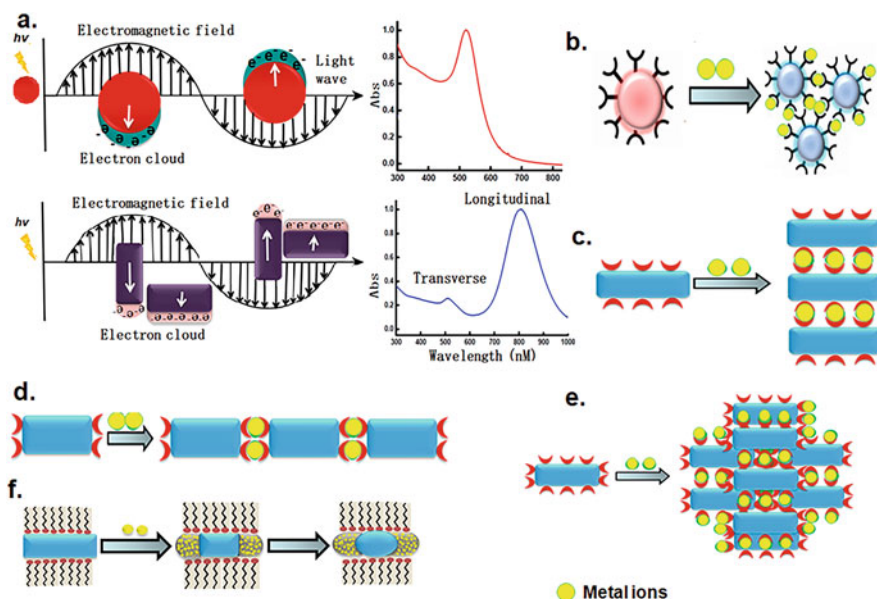
Fig. 12.4 Schematic illustration of surface plasmon excitation of GNP and GNR (**a**), metal ion-mediated aggregation of GNP (**b**); metal ion-induced side by side (**c**), end to end interaction (**d**), both side by side and end to end interaction forming total aggregate of GNR (**e**), and metal ion-mediated etching of GNR to spherical-shaped nanoparticle (**f**) responsible for the change in optical properties of gold nanostructures

Thus, a change in SPR band can be used to track the interaction of analytes with gold nanoparticles (Nath et al. 2018b).

The detection mechanism of colorimetric sensors is dependent on the change in color and absorption band associated with the aggregation and disaggregation of nanoparticles. Interaction of heavy metals with spherical gold nanoparticles forms aggregates with a shift in SPR and red to blue color change (Fig. 12.4b). However, gold nanorod aggregates in different ways, namely end to end, side by side, aggregation, and etching of nanorod (Vigderman et al. 2012). End to end interaction occurs when metal toxins bind at the edge of nanorod forming chain/wire-like structure resulting in bathochromic shift of longitudinal band. Metals toxins when bound on the longer edge of the nanorod result in side by side interaction with a blue shift in longitudinal SPR. Aggregation-based assembly first initiates with end to end and ends side by side, forming a total-aggregate nanorod with decreased absorption band intensity. Some metal toxins etch nanorod at longitudinal edge forming spherical shape coupled with red shift and change in color from purple to pink. The change in optical properties with toxic ion-mediated aggregation has been shown in Fig. 12.4c, d, e, f.

12.5 GNP as a Colorimetric Sensor for Heavy Metals

As discussed in Sect. 12.4.3, gold nanoparticles are extremely responsive to the local dielectric, which results in aggregation with change in SPR and the color of colloidal solution indicating the presence of test analyte. Researchers have extensively investigated this feature to develop a color-based sensor for metal ions, which has been discussed in this section. Chen et al. reported DMSA functionalized GNP for trace level detection of $Cr^{III/VI}$. Chromium exists as an aqueous complex with six water molecules coordinated with the Cr^{III} ion. Cr(III) has empty orbitals that accept one pair of electrons from the oxygen of DMSA, forming a metal–O coordinate covalent bond by replacing water molecules from aqueous chromium. However, in the case of $Cr_2O_7^{2-}$, the Cr^{VI} ion lacks coordination sites as they are already occupied by oxygen atoms. Therefore, chromium binding occurs through hydrogen bonding OH----O involving carboxyl –OH of DMSA and –O of $Cr_2O_7^{2-}$ (Fig. 12.5a). (Chen et al. 2015) Nath et al. reported a red to blue color change sensor for arsenic (III and V) using 2-mercapto-4-methyl-5-thiazoleacetic acid (MMT) and
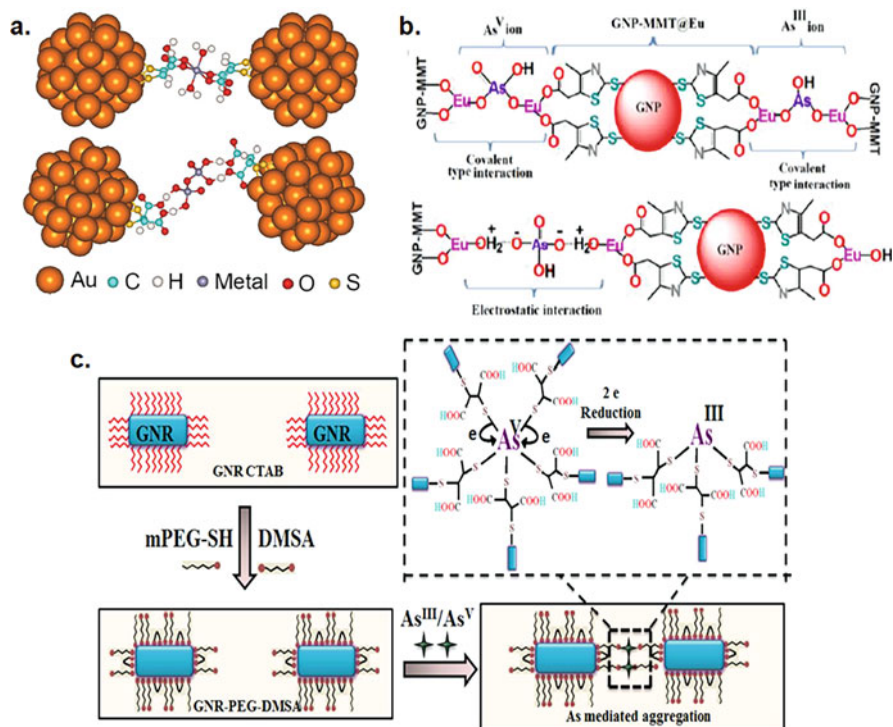

Fig. 12.5 (a) Interactions between DMSA-GNP and Cr^{III} (top) and Cr^{VI} (down). (b) $As^{III/V}$ mediated aggregation of GNP-MMT@Eu. (c) $As^{III/V}$ induced aggregation of DMSA functionalized gold nanorod. Reproduced from Ref. Chen et al. (2015)) (a). Reproduced from Ref. Nath et al. (2018a)) (b). Reproduced from Ref. Priyadarshni et al. (2018) (c)

europium chloride ($EuCl_3$) functionalized gold nanoparticle (GNP-MMT@Eu). The SPR peak intensity of GNP-MMT@Eu at 525 nm decreased while a new peak at 650 nm appeared due to arsenic-mediated aggregation of nanosensor. GNP-MMT@Eu exhibits Eu-OH group exposed on GNP surface which are the sole binding sites for arsenic ion. The As-OH/As-O$^-$ groups of arsenic and –OH groups of Eu(III) bind forming an inner-sphere arsenic complex between GNP with the release of H_2O and OH$^-$ moieties. The response of GNP-MMT@Eu for As (V) was quick compared to that of As(III). The nanosensor surface attains a partial positive charge at pH ~6-7 as the Eu-OH converts to Eu-OH$_2^+$ which initiates the binding between $H_2AsO_4^-$/$HAsO_4^{2-}$ and GNP-MMT@Eu through electrostatic interaction. Thus, both covalent and electrostatic modes of binding prevail between arsenic and the nanosensor, which are accountable for rapid response to As^V (Fig. 12.5b) (Nath et al. 2018a). Priyadarshni et al. demonstrated aggregation-based detection of As$^{III/V}$ using gold nanorod (GNR) modified with mPEG-SH and DMSA. After interaction with As$^{III/V}$, the bluish-purple color of the GNR sensor turns colorless with a small shift (778 to ~802-820 nm) and decrease in SPR peak suggesting side to side and end to end binding forming total aggregate. DMSA contains two thiols (–SH) groups; one binds with GNR and other complexes with As$^{III/V}$. At pH ~7, As^{III} and As^V exist as H_3AsO_3 and H_3AsO_4/$H_2AsO_4^-$ while thiol remains protonated. As−OH groups participate in As−S bond formation and release H_2O due to removal of hydrogen from –SH and displacement of –OH$^-$ to form a complex between As$^{III/V}$ and GNR, inducing arsenic-mediated aggregation of nanorods (Fig. 12.5c) (Priyadarshni et al. 2018).

12.5.1 Detection on Paper Substrate

Conventional detection methods for metal toxins have constantly improvised with new-age technological developments to miniaturize the setup and provide a decentralized approach. The emergence of microfluidic techniques resulted in the notion of the "lab-on-chip (LOC)" concept back in the 1990s (Guan and Sun 2020; Sackmann et al. 2014). In recent years, paper-based microfluidics have emerged as promising LOC sensing devices (Li et al. 2012; Yetisen et al. 2013; Kumar et al. 2015). Microfluidics that couple paper-based devices with colorimetric analysis are particularly attractive, attributed to easy fabrication, portability, and inexpensive, i.e., provide a cheaper alternative for point-of-use testing. Moreover, the paper has a porous matrix that offers self-pumping and capillary flow to the solution (Mahato et al. 2020; Xiong et al. 2020; Mahato et al. 2017). This section discusses some paper-based colorimetric methods for sensing toxic metal ions in water. Nath et al. reported trace-level determination of As^{III} on Y-shaped microfluidic paper device using thioctic acid and thioguanine conjugated gold nanoparticle (Au-TA-TG). The two arms of the device were used as the inlet, each for Au-TA-TG and As^{III}, and the reaction occurs on the paper surface resulting in red to blue color change, suggesting the existence of As^{III} (Fig. 12.6a) (Nath et al. 2014). Zhang and coworkers demonstrated the detection of Cu^{II} by etching of nanorod in the presence of
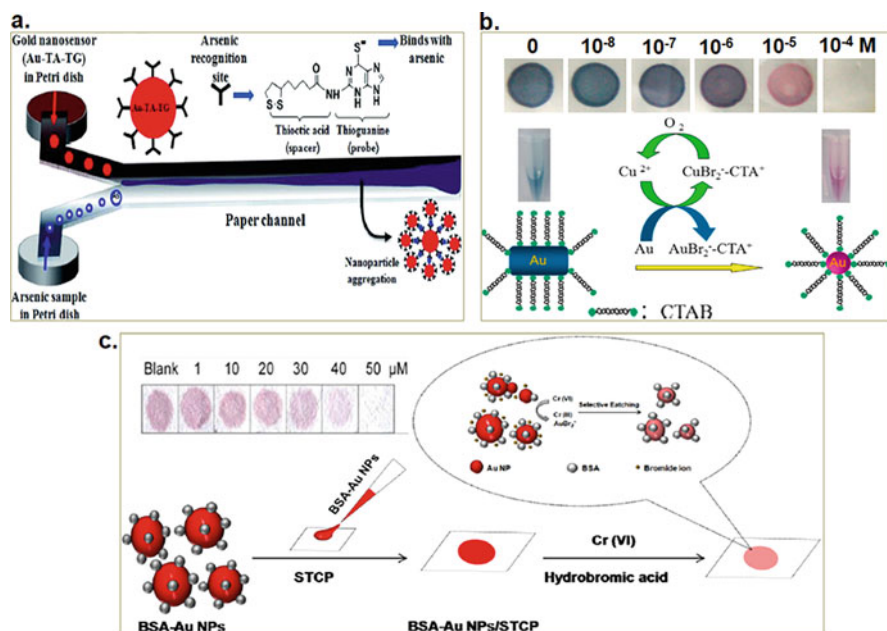
Fig. 12.6 (**a**) Au-TA-TG on Y-shaped paper strip for colorimetric detection of As^{III}. (**b**) Paper-based colorimetric detection of Cu^{II} by etching of nanorod in the presence of HBr turns blue-to-red. (**c**) Paper-based colorimetric detection of Cr^{VI} by aggregation of BSA-AuNP/STCP. Reproduced from Ref. Nath et al. (2014)) (**a**). Reproduced from Ref. Zhang et al. (2014) (**b**). Reproduced from Ref. Guo et al. (2016) (**c**)

hexadecyltrimethylammonium bromide (HBr) on a paper substrate. When Cu^{II} in combination with HBr is added to nanorod, HBr induces transformation of Au(0)-to-Au(I) and Cu^{II} catalytically etches the longitudinal edge of GNR accompanied with color change from blue to red (Fig. 12.6b) (Zhang et al. 2014). Paper-based colorimetric metal ion detection using gold nanoparticles has been shown in Fig. 12.6 and listed in Table 12.2.

12.6 Smartphone and Machine Learning (Color Readout)-Based Quantification of Heavy Metals

The enhanced technical capabilities of smartphones, especially wireless connectivity and high definition cameras, enable various innovative ideas for detecting environmental toxins like heavy metals (Mutlu et al. 2017). The addition of a simple colorimetric sensing apparatus to a smartphone makes it lab-on-phone, cost-effective, portable, and accurate (Sajed et al. 2020; Wang et al. 2019). Most of the integrated smartphone detection systems introduced so far rely on RGB (red, green, blue) intensities of the colorimetric sensor. Chen et al. developed a smartphone integrated colorimetric sensor using meso-2,3-dimercaptosuccinic acid

Table 12.2 GNP- and GNR-mediated colorimetric detection of metal toxins in solution, paper substrate, and smartphone

Target metal toxin	Modification	LOD (ppb)	Aggregation-based color change of GNP/GNR	Ref
Arsenic				
GNP	Glutathione(GSH), Dithiothreitol (DTT) cysteine (Cys)	1.0	Red→blue	Kalluri et al. (2009)
	Aptamer	1.26	Red → blue	Yu (2014)
	GSH-DTT-Cys-PDCA	2.5	Red →blue	Domínguez-González et al. (2014)
	Cationic polymer and aptamer	5.3	Red → blue	Wu et al. (2012)
	Citrate	1.8	Red → blue	Gong et al. (2017)
	Polyethyleneglycol (PEG)	5.0	Red→ blue	Boruah and Biswas (2018)
	Thioctic acid-thioguanine (TA-TG)	1.0	Paper-based; red→blue	Nath et al. (2014)
	2-mercapto-4-methyl-5-thiazoleacetic acid (MMT)- europium	1.0	Paper-based; red→blue	Nath et al. (2018a)
	Sucrose	4.0	Smartphone-based color intensity extraction using ImageJ software; red→blue	Shrivas et al. (2020)
	Glutathione (GSH)	0.12	Smartphone-based RGB extraction; red→blue	Zheng et al. (2021)
GNR	Meso 2,3-Dimercaptosuccinic acid (DMSA)	1.0	Paper-based; purple→colorless	Priyadarshni et al. (2018)
Chromium				
GNP	5,5′-dithiobis (2-nitrobenzoic acid) (DTNBA	93.6	Red →blue	Dang et al. (2009)
	Triazole	72.6	Red →blue	Chen et al. (2013)
	Citrate	15.5	Red →blue	Liu and Wang (2013)
	Citrate	5.3	Paper-based; red →blue	Elavarasi et al. (2013)
	Tween 20	Cr^{III}: 0.83 Cr^{VI}: 0.46	Red →blue	Wang et al. (2015)
	4-amino hippuric acid.	60.7	Red →blue	Jin and Huang (2017)

(continued)

Table 12.2 (continued)

Target metal toxin	Modification	LOD (ppb)	Aggregation-based color change of GNP/GNR	Ref
	Gallic acid	78	Red →blue	Dong et al. (2016)
	O-phospho-l-serine dithiocarbamic acid (PSDTC)	218	Red →blue	Lo et al. (2015)
	1,5-diphenylcarbazide (DPC)	15.5	Red →blue	Liu et al. (2016)
	Cysteamine-pyridoxal (CAPY)	596.9	Red →blue	Bothra et al. (2017)
	Ribavirin	1.55	Red →blue	Salimi et al. (2018)
	Thiol modified nanodiamonds (ND-thiol)	0.019	Red →blue	Shellaiah et al. (2018)
	Bovine serum albumin (BSA)	14.5	Paper-based; red →blue	Guo et al. (2016)
	Meso-2,3-dimercaptosuccinic Acid (DMSA)	0.51	Smartphone readout; red→blue	Chen et al. (2015)
GNR	Bovine serum albumin (BSA)	16.6	Purple→red (etching)	Alex et al. (2018)
Lead				
GNP	Glutathione	0.002	Red →blue	Chai et al. (2010)
	L-glutathione	0.1 umol/L	Red →blue	Mao et al. (2011)
	Maleic acid	0.5	Red →blue	Ratnarathorn et al. (2015)
	Thioctic acid (TA--Dansyl hydrazine (DNS)	1.0	Paper-based; red →blue	Nath et al. (2015)
	Oligonucleotide	0.5	Smartphone-based RGB extraction and machine learning; red→blue	Sajed et al. (2020)
GNR	Cysteine	0.02	Absorption Side-by-side assembly	Cai et al. (2014)
	Unmodified GNR	0.62	Etching of GNR and Pb-au alloy formation	Chen et al. (2012)
	Sodium thiosulfate	20.7	Blue→red (etching of GNR)	Zhu et al. (2016)
Mercury				
GNP	Papain	0.2	Red →blue	Guo et al. (2011)
	3-mercaptopropionate acid and adenosine monophosphate	0.5	Red →blue	Yu and Tseng (2008)

Table 12.2 (continued)

Target metal toxin	Modification	LOD (ppb)	Aggregation-based color change of GNP/GNR	Ref
	2-[3-(2-aminoethylsulfanyl)-Propylsulfanyl]- ethylamine (AEPE)	0.035	Red →blue	Chansuvarn and Imyim (2012)
	Thioctic acid (TA)	0.01	Red →blue	Su et al. (2013)
	Label-free oligonucleotide	0.05	Red →blue	Lee and Mirkin (2008)
	ss-DNA	10	µPAD integrated with smartphone (RGB values); red→blue	Chen et al. (2014a)
	Aptamer	0.2	Smartphone-based RGB extraction and machine learning; red→blue	Sajed et al. (2019)
GNR	Pyrazole	0.002	Absorption and colorimetric (end to end assembly)	Placido et al. (2013)
	Dithiothretol (DTT)	0.08	Absorption and colorimetric (aggregation)	Bi et al. (2012)
	Silica-CN	1.08	Colorimetric (au-hg amalgamation)	Anand et al. (2013)
	Mesoporous silica	0.15	Redox mediated inner particle interaction	
Copper				
GNP	Dopamine dithiocarbamate decorated gold nanoparticles (DDTC-au NPs)	946.2	Red →blue	Mehta et al. (2013)
	Polyvinylpyrrolidone (PVP) aggregated with 2-Mercaptobenzimidazole (MBI)	317.5	Purple→red (dis-aggregation)	Ye et al. (2015)
	10-mercaptodecyl-1-iminodiacetic acid (MDIA)	508	Red →blue	Chai et al. (2017)
	Amyloid-like peptides (arginine, phenylalanine, proline)	7.62	Red →blue	Pelin et al. (2020)
	Thioctic acid (TA--Dansyl hydrazine (DNS)	1.0	Paper-based; red →blue	Nath et al. (2015)
GNR	Cysteine	0.02	Blue-green→dark gray (aggregation)	Liu et al. (2011)
	Hexadecyltrimethylammonium bromide	0.03	Paper-based; blue→red (etching)	Zhang et al. (2014)

Table 12.2 (continued)

Target metal toxin	Modification	LOD (ppb)	Aggregation-based color change of GNP/GNR	Ref
Cadmium				
GNP	6-mercaptonicotinic acid (MNA) and L-cysteine (LCys)	11.2	Red →blue	Xue et al. (2011)
	4-amino-3-hydrazino-5-mercapto-1,2,4-triazole (AHMT)	3.37	Red →blue	Wang et al. (2013)
	2,6-dimercaptopurine	3.67	Red →blue	Gan et al. (2020)

(DMSA)-capped GNP to detect chromium ions (III and VI). The detection system was dependent on RGB extraction using an application software "color scan" and the ratio of green to red was calculated to obtain a calibration curve and determine the amount of chromium in the real water sample (Fig. 12.7a) (Chen et al. 2015). Faham and coworkers showed a paper-based colorimetric sensor integrated with smartphone readout for chromium (III) detection in solution. 2,2′-thiodiacetic acid-modified gold nanoparticle (TDA-GNP) was spotted on a paper disc and treated with various concentrations of Cr^{III} followed by image capturing using a Samsung E5 smartphone. Color intensities of the paper disc were obtained using adobe photoshop CS5 and applied to obtain Cr^{III} concentration in real samples (Faham et al. 2018). Smartphone-based detection provides real-time on-site application of colorimetric sensors with the help of simple software available by third-party service providers. However, to obtain analytical values from color, the images are highly processed and compressed, leading to alterations in final analytical data and cannot be trusted completely. Moreover, simple analytical models fail to detect the number of independent variables like in the multi-analyte sensor. The drawbacks of illumination and smartphone detection systems can be overcome by applying artificial intelligent systems like machine learning (Mutlu et al. 2017).

Machine learning (ML) is a subset of artificial intelligence (AI) that acquires information from raw data by extracting its features and uses it to tackle problems without human intervention. It is a computer program or algorithm that makes machines more intelligent in behavior and decision by enabling them to learn from past experiences and develop their own program (Cui et al. 2020; Lussier et al. 2020). In the field of sensing, ML is employed as a tool for data processing to extract features like color intensity and utilize these features to predict the concentration of analyte and toxic ions directly (Cui et al. 2020). A general workflow of machine learning and its advantages in colorimetric sensing is presented in Fig. 12.7b. ML is grouped into two classes: supervised and unsupervised learning (Ayodele 2010). In unsupervised learning, the algorithm is not trained with the input data (training data);
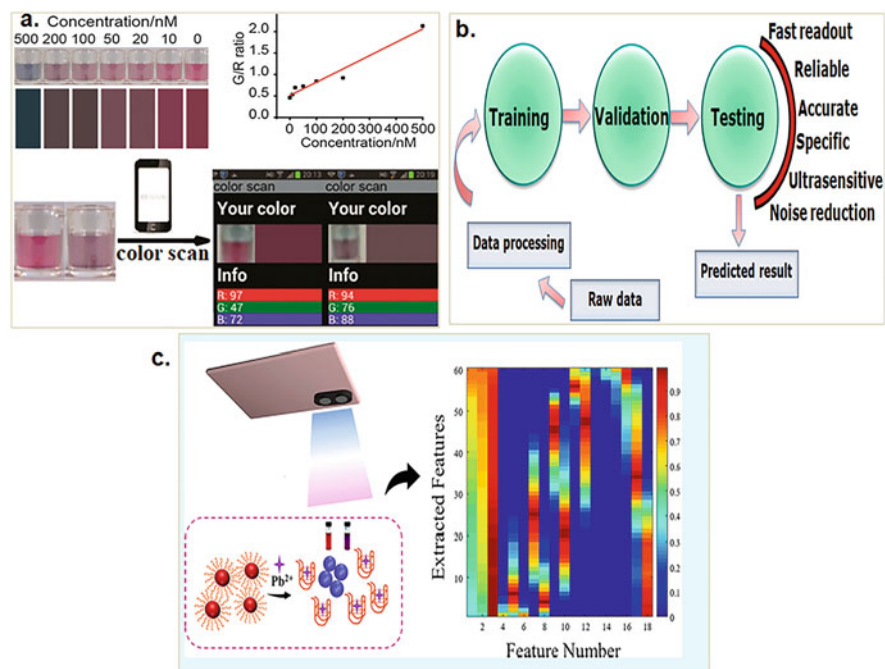
Fig. 12.7 (**a**) RGB extraction and smartphone readout-based detection of Cr$^{III/VI}$ using DMSA-GNP. (**b**) General work flow of machine learning and its advantages in colorimetric sensing. (**c**) Smartphone readout and regression-based model to process RGB features extracted from color change on interaction of Pb^{II} with oligonucleotide-GNP. Reproduced from Ref. Chen et al. (2015) (**a**). Reproduced from Ref. Sajed et al. (2020) (**c**)

instead, it learns from the pattern of untagged data, builds a concept, and predicts the output. k-Means clustering is the most used unsupervised learning algorithm.

On the contrary, supervised learning involves training of ML algorithms with input data called training data. Based on training data, the algorithm predicts the output for the unknown input data called testing data. Convolutional neural network (CNN), artificial neural network (ANN), support vector machine (SVM), and multiple linear regression (MLR) are some supervised ML algorithms, gaining attention in chemical and biological colorimetric sensors development (Cui et al. 2020). Sajed group reported a novel detection method for Hg^{II} ions in water utilizing smartphone-based machine learning regression. Aptamer modified gold nanoparticle changes color from red to purple in Hg^{II}, and the corresponding color change was captured on a smartphone camera. The obtained color cards trained the machine learning regression model to interpret mercury ion concentration based on RGB values. The smartphone was fabricated with an optoelectronic component using three-dimensional printing technology, an attachment to any smartphone. The optoelectronic device comprises three compartments: LCD board and camera's depth focus chamber, and cuvette holder. This setup provides an advantage of

blocking ambient light interference and results in reproducible LCD illumination (Sajed et al. 2019). In another work, Sajed et al. reported similar detection apparatus for Pb^{II} ion using oligonucleotide modified gold nanoparticle and machine learning regression on the mobile platform (Fig. 12.7c) (Sajed et al. 2020). Machine learning combined with a smartphone provides high sensitivity, accuracy, and easy operation with ubiquitous detection using Lab-on-phone apparatus.

12.7   Conclusion

Metal nanoparticle-based colorimetric sensing has gained special attention in the detection of environmental toxins because of distinct chemical and optical characteristics, including catalytic behavior, easy synthesis, and a broad array of surface functionalization molecules. SPR-based color change associated with the aggregation of nanoparticles is the primary mechanism to develop a colorimetric sensor. Gold and silver nanoparticles exhibit distinct SPR features. On the other hand, the platinum-type nanoparticle is explored mainly for its catalytic activity and enzyme mimetic behavior to induce an indirect color change in sensing application. Among all these metallic nanoparticles, gold nanoparticles (GNP) have emerged as a versatile platform for detecting toxic metal ions because of their stability, ease of synthesis, and functionalization with biomolecules and unique optical properties. Compared to traditional methods, GNP-based colorimetric sensor provides rapid and inexpensive detection techniques specifically for the metal toxins with a detection limit of micro-to-pico molar level. Recently, a paper-based analytical device coupled with colorimetric assay emerged as a cheaper alternative to conventional methods to develop the point-of-use testing system. This technique involves immobilization of modified gold nanoparticles on paper, and metal toxins are allowed to flow through it, exploring the self-wicking property of paper substrate toward metal ion detection. The paper-based colorimetric devices provide a field-deployable miniaturized sensing platform. The developments in sensing strategies have given a new lab-on-phone concept, which includes the addition of a simple colorimetric sensing apparatus to a smartphone. This smartphone-based sensing apparatus relies on RGB (red, green, blue) features extracted from the color intensities of samples. However, the images become highly processed and compressed during feature extraction, and thus results from the smartphone-based devices cannot be trusted completely. The drawbacks of smartphone detection systems can be overcome by applying artificial intelligence systems like machine learning algorithms. ML is employed as a tool for data processing to extract features like color intensity and utilize these features to predict the concentration of toxic metal ions directly in the field of sensing.

References

Alam AU, Clyne D, Jin H, Hu NX, Deen MJ (2020) Fully integrated, simple, and low-cost electrochemical sensor Array for in situ water quality monitoring. ACS Sensors 5:412–422. https://doi.org/10.1021/acssensors.9b02095

Aldewachi H, Chalati T, Woodroofe MN, Bricklebank N, Sharrack B, Gardiner P (2018) Gold nanoparticle-based colorimetric biosensors. Nanoscale 10:18–33. https://doi.org/10.1039/c7nr06367a

Alex SA, Chandrasekaran N, Mukherjee A (2018) Centre for nanobiotechnology CR. J Mol Liq. https://doi.org/10.1016/j.molliq.2018.05.056

Amina SJ, Guo B (2020) A review on the synthesis and functionalization of gold nanoparticles as a drug delivery vehicle. Int J Nanomedicine 15:9823–9857. https://doi.org/10.2147/IJN.S279094

Anand GS, Gopalan AI, Kang S-W, Lee K-P (2013) Development of a surface plasmon assisted label-free calorimetric method for sensitive detection of mercury based on functionalized gold nanorods. J Anal At Spectrom 28:488–498. https://doi.org/10.1039/C3JA30300D

Annadhasan M, Muthukumarasamyvel T, Sankar Babu VR, Rajendiran N (2014) Green synthesized silver and gold nanoparticles for colorimetric detection of Hg2+, Pb2+, and Mn2+ in aqueous medium. ACS Sustain Chem Eng 2:887–896. https://doi.org/10.1021/sc400500z

Ayodele TO (2010) Types of machine learning algorithms. In: Zhang Y (ed) New advances in machine learning. IntechOpen, Rijeka

Balasurya S, Syed A, Thomas AM, Marraiki N, Elgorban AM, Raju LL, Das A, Khan SS (2020) Rapid colorimetric detection of mercury using silver nanoparticles in the presence of methionine. Spectrochim Acta Part A Mol Biomol Spectrosc 228:117712. https://doi.org/10.1016/j.saa.2019.117712

Baranwal A, Mahato K, Srivastava A, Maurya PK, Chandra P (2016) Phytofabricated metallic nanoparticles and their clinical applications. RSC Adv 6:105996–106010. https://doi.org/10.1039/C6RA23411A

Bertolacci L, Valentini P, Pompa PP (2020) A nanocomposite hydrogel with catalytic properties for trace-element detection in real-world samples. Sci Rep 10:18340. https://doi.org/10.1038/s41598-020-75103-8

Bi N, Chen Y, Qi H, Zheng X, Chen Y, Liao X, Zhang H, Tian Y (2012) Spectrophotometric determination of mercury(II) ion using gold nanorod as probe. Sensors Actuators B Chem 166–167:766–771. https://doi.org/10.1016/j.snb.2012.03.068

Boruah BS, Biswas R (2018) Selective detection of arsenic ({III}) based on colorimetric approach in aqueous medium using functionalized gold nanoparticles unit. Mater Res Express 5:15059. https://doi.org/10.1088/2053-1591/aaa661

Boruah BS, Daimari NK, Biswas R (2019) Functionalized silver nanoparticles as an effective medium towards trace determination of arsenic (III) in aqueous solution. Results Phys 12:2061–2065. https://doi.org/10.1016/j.rinp.2019.02.044

Bothra S, Kumar R, Sahoo SK (2017) Pyridoxal conjugated gold nanoparticles for distinct colorimetric detection of chromium(iii) and iodide ions in biological and environmental fluids. New J Chem 41:7339–7346. https://doi.org/10.1039/C7NJ00350A

Brust M, Walker M, Bethell D, Schiffrin DJ, Whyman R (1994) Synthesis of thiol-derivatised gold nanoparticles in a two-phase Liquid–Liquid system. J Chem Soc Chem Commun 1994:801–802. https://doi.org/10.1039/C39940000801

Buledi JA, Amin S, Haider SI, Bhanger MI, Solangi AR (2020) A review on detection of heavy metals from aqueous media using nanomaterial-based sensors. Environ Sci Pollut Res. https://doi.org/10.1007/s11356-020-07865-7

Cai H-H, Lin D, Wang J, Yang P-H, Cai J (2014) Controlled side-by-side assembly of gold nanorods: a strategy for lead detection. Sensors Actuators B Chem 196:252–259. https://doi.org/10.1016/j.snb.2014.01.062

Chai F, Wang C, Wang T, Li L, Su Z (2010) Colorimetric detection of Pb2+ using glutathione functionalized gold nanoparticles. ACS Appl Mater Interfaces 2:1466–1470. https://doi.org/10.1021/am100107k

Chai W, Feng Q, Nie M, Wang C, Jiang Y, Zheng H, Li MJ (2017) Gold nanoparticle-based probe for colorimetric detection of copper ions. J Nanosci Nanotechnol 17:502–506. https://doi.org/10.1166/jnn.2017.12419

Chang HH, Murphy CJ (2018) Mini gold Nanorods with tunable Plasmonic peaks beyond 1000 nm. Chem Mater 30:1427–1435. https://doi.org/10.1021/acs.chemmater.7b05310

Chansuvarn W, Imyim A (2012) Visual and colorimetric detection of mercury(II) ion using gold nanoparticles stabilized with a dithia-diaza ligand. Microchim Acta 176:57–64. https://doi.org/10.1007/s00604-011-0691-3

Chen G, Jin Y, Wang W, Zhao Y (2012) Colorimetric assay of lead using unmodified gold nanorods. Gold Bull 45:137–143. https://doi.org/10.1007/s13404-012-0057-6

Chen GH, Chen WY, Yen YC, Wang CW, Chang HT, Chen CF (2014a) Detection of mercury (II) ions using colorimetric gold nanoparticles on paper-based analytical devices. Anal Chem 86:6843–6849. https://doi.org/10.1021/ac5008688

Chen L, Li J, Chen L (2014b) Colorimetric detection of mercury species based on functionalized gold nanoparticles. ACS Appl Mater Interfaces. https://doi.org/10.1021/am503531c

Chen W, Cao F, Zheng W, Tian Y, Xianyu Y, Xu P, Zhang W, Wang Z, Deng K, Jiang X (2015) Detection of the nanomolar level of total Cr[(III) and (VI)] by functionalized gold nanoparticles and a smartphone with the assistance of theoretical calculation models. Nanoscale 7:2042–2049. https://doi.org/10.1039/c4nr06726f

Chen W, Fang X, Li H, Cao H, Kong J (2016) 0.1038/srep 31948.Er-based colorimetric device for rapid mercury(II) assay. Sci Rep 6:1–7. https://doi.org/10.1038/srep31948

Chen Y, Lee I, Sung Y, Wu S (2013) Sensors and actuators B: chemical Triazole functionalized gold nanoparticles for colorimetric Cr 3 + sensing. Sensors Actuators B Chem 188:354–359. https://doi.org/10.1016/j.snb.2013.06.088

Cheon JY, Park WH (2016) Green synthesis of silver nanoparticles stabilized with mussel-inspired protein and colorimetric sensing of Lead(II) and copper(II) ions. Int J Mol Sci 17:2006. https://doi.org/10.3390/ijms17122006

Choi J, Park S, Stojanović Z, Han HS, Lee J, Seok HK, Usković D, Lee KH (2013) Facile solvothermal preparation of monodisperse gold nanoparticles and their engineered assembly of ferritin-gold nanoclusters. Langmuir 29:15698. https://doi.org/10.1021/la403888f

Cui F, Yue Y, Zhang Y, Zhang Z, Zhou HS (2020) Advancing biosensors with machine learning. ACS Sensors 5:3346–3364. https://doi.org/10.1021/acssensors.0c01424

Dang Y, Li H, Wang B, Li L, Wu Y (2009) Selective detection of trace Cr 3 + in aqueous solution by using 5,5′-Dithiobis (2-Nitrobenzoic acid)-modified gold nanoparticles. ACS Appl Mater Interfaces 1:1533–1538. https://doi.org/10.1021/am9001953

Das RK, Gogoi N, Bora U (2011) Green synthesis of gold nanoparticles using Nyctanthes arbortristis flower extract. Bioprocess Biosyst Eng 34:615–619. https://doi.org/10.1007/s00449-010-0510-y

Divsar F, Habibzadeh K, Shariati S, Shahriarinour M (2015) Aptamer conjugated silver nanoparticles for the colorimetric detection of arsenic ions using response surface methodology. Anal Methods 7:4568–4576. https://doi.org/10.1039/C4AY02914C

Domínguez-González R, González Varela L, Bermejo-Barrera P (2014) Functionalized gold nanoparticles for the detection of arsenic in water. Talanta 118:262–269. https://doi.org/10.1016/j.talanta.2013.10.029

Dong C, Wu G, Wang Z, Ren W, Zhang Y, Shen Z, Li T, Wu A (2016) Selective colorimetric detection of Cr(III) and Cr(VI) using gallic acid capped gold nanoparticles. Dalt Trans 45:8347–8354. https://doi.org/10.1039/c5dt04099j

Doria G, Conde J, Veigas B, Giestas L, Almeida C, Assunção M, Rosa J, Baptista PV (2012) Noble metal nanoparticles for biosensing applications. Sensors 12:1657–1687. https://doi.org/10.3390/s120201657

Elavarasi M, Rajeshwari A, Chandrasekaran N, Mukherjee A (2013) Simple colorimetric detection of Cr(iii) in aqueous solutions by as synthesized citrate capped gold nanoparticles and development of a paper based assay. Anal Methods 5:6211–6218. https://doi.org/10.1039/c3ay41435c

Epifani M, Giannini C, Tapfer L, Vasanelli L (2000) Sol-gel synthesis and characterization of ag and au nanoparticles in SiO2, TiO2, and ZrO2 thin films. J Am Ceram Soc 83:2385. https://doi.org/10.1111/j.1151-2916.2000.tb01566.x

Faham S, Khayatian G, Golmohammadi H, Ghavami R (2018) A paper-based optical probe for chromium by using gold nanoparticles modified with 2,2′-thiodiacetic acid and smartphone camera readout. Microchim Acta 2018:185. https://doi.org/10.1007/s00604-018-2875-6

Firdaus M, Fitriani I, Wyantuti S, Hartati Y, Khaydarov R, MCalister J, Obata H, Gamo T (2017) Colorimetric detection of mercury(II) ion in aqueous solution using silver nanoparticles. Anal Sci 33:831–837. https://doi.org/10.2116/analsci.33.831

Gan Y, Liang T, Hu Q, Zhong L, Wang X, Wan H, Wang P (2020) In-situ detection of cadmium with aptamer functionalized gold nanoparticles based on smartphone-based colorimetric system. Talanta 208:120231. https://doi.org/10.1016/j.talanta.2019.120231

Gao X, Lu Y, He S, Li X, Chen W (2015) Colorimetric detection of iron ions (III) based on the highly sensitive plasmonic response of the N-acetyl-l-cysteine-stabilized silver nanoparticles. Anal Chim Acta 879:118–125. https://doi.org/10.1016/j.aca.2015.04.002

Ghosh P, Han G, De M, Kim CK, Rotello VM (2008) Gold nanoparticles in delivery applications. Adv. Drug Deliv. Rev 60:1307

Gong L, Du B, Pan L, Liu Q, Yang K, Wang W, Zhao H, Wu L, He Y (2017) Colorimetric aggregation assay for arsenic(III) using gold nanoparticles. Microchim Acta 184:1185–1190. https://doi.org/10.1007/s00604-017-2122-6

Guan Y, Sun B (2020) Detection and extraction of heavy metal ions using paper-based analytical devices fabricated via atom stamp printing. Microsystems Nanoeng 6:14. https://doi.org/10.1038/s41378-019-0123-9

Guo J, Huo D, Mei Y, Hou C, Li J, Fa H, Luo H, Yang P (2016) Colorimetric detection of Cr (VI) based on the leaching of gold nanoparticles using a paper-based sensor. Talanta 161:198–185. https://doi.org/10.1016/j.talanta.2016.09.032

Guo L, Mao L, Huang K, Liu H (2017) Pt–se nanostructures with oxidase-like activity and their application in a selective colorimetric assay for mercury(II). J Mater Sci 52:10738–10750. https://doi.org/10.1007/s10853-017-1181-8

Guo Y, Wang Z, Qu W, Shao H, Jiang X (2011) Colorimetric detection of mercury, lead and copper ions simultaneously using protein-functionalized gold nanoparticles. Biosens Bioelectron 26:4064–4069. https://doi.org/10.1016/j.bios.2011.03.033

He S, Lin X, Liang H, Xiao F, Li F, Liu C, Fan P, Yang S, Liu Y (2019) Colorimetric detection of Cr (vi) using silver nanoparticles functionalized with PVP. Anal Methods 11:5819–5825. https://doi.org/10.1039/C9AY02010A

Huang P, Liu B, Jin W, Wu F, Wan Y (2016) Colorimetric detection of Cd2+ using 1-amino-2-naphthol-4-sulfonic acid functionalized silver nanoparticles. J Nanopart Res 18:327. https://doi.org/10.1007/s11051-016-3630-8

Husseiny M, El-Aziz M, Badr Y, Mahmoud M (2007) Biosynthesis of gold nanoparticles using pseudomonas aeruginosa. Spectrochim Acta Part A 67:1003–1006. https://doi.org/10.1063/1.2711108

Iravani S (2011) Green synthesis of metal nanoparticles using plants. Green Chem 13:2638–2650. https://doi.org/10.1039/C1GC15386B

Isildak Ö, Özbek O (2020) Application of potentiometric sensors in real samples. Crit Rev Anal Chem 0:1–14. https://doi.org/10.1080/10408347.2019.1711013

Ismail M, Khan M, Akhtar K, Khan M, Asiri AM, Khan S (2018) Biosynthesis of silver nanoparticles: a colorimetric optical sensor for detection of hexavalent chromium and ammonia in aqueous solution. Phys E Low-dimensional Syst Nanostructures 103:367–376. https://doi.org/10.1016/j.physe.2018.06.015

Jana NR, Gearheart L, Murphy CJ (2001) Wet chemical synthesis of high aspect ratio cylindrical gold nanorods. J Phys Chem B 105:4065–4067. https://doi.org/10.1021/jp0107964

Jans H, Huo Q (2012) Gold nanoparticle-enabled biological and chemical detection and analysis. Chem Soc Rev 41:2849–2866. https://doi.org/10.1039/c1cs15280g

Jayabal S, Pandikumar A, Lim HN, Ramaraj R, Sun T, Huang NM (2015a) A gold nanorod-based localized surface plasmon resonance platform for the detection of environmentally toxic metal ions. Analyst 140:2540–2555. https://doi.org/10.1039/c4an02330g

Jayabal S, Pandikumar A, Lim HN, Ramaraj R, Sun T, Huang NM (2015b) A gold nanorod-based localized surface plasmon resonance platform for the detection of environmentally toxic metal ions. Analyst 140:2540–2555. https://doi.org/10.1039/C4AN02330G

Jeevika A, Ravi Shankaran D (2014) Visual colorimetric sensing of copper ions based on reproducible gelatin functionalized silver nanoparticles and gelatin hydrogels. Colloids Surfaces A Physicochem Eng Asp 461:240–247. https://doi.org/10.1016/j.colsurfa.2014.08.002

Jin W, Huang P (2017) Colorimetric detection of Cr3 + using gold nanoparticles functionalized with 4- amino hippuric acid colorimetric detection of Cr 3 + using gold nanoparticles functionalized with 4-amino hippuric acid. J Nanopart Res 17:1–10. https://doi.org/10.1007/s11051-015-3156-5

Jin W, Huang P, Wu F, Ma L-H (2015) Ultrasensitive colorimetric assay of cadmium ion based on silver nanoparticles functionalized with 5-sulfosalicylic acid for wide practical applications. Analyst 140:3507–3513. https://doi.org/10.1039/C5AN00230C

Joshi P, Sarkar S, Soni SK, Kumar D (2016) Label-free colorimetric detection of Cr(VI) in aqueous systems based on flower shaped silver nanoparticles. Polyhedron 120:142–149. https://doi.org/10.1016/j.poly.2016.07.037

Kalluri JR, Arbneshi T, Afrin Khan S, Neely A, Candice P, Varisli B, Washington M, McAfee S, Robinson B, Banerjee S, Singh AK, Senapati D, Ray PC (2009) Use of gold nanoparticles in a simple colorimetric and ultrasensitive dynamic light scattering assay: selective detection of arsenic in groundwater. Angew Chemie Int Ed 48:9668–9671. https://doi.org/10.1002/anie.200903958

Khandel P, Yadaw RK, Soni DK, Kanwar L, Shahi SK (2018) Biogenesis of metal nanoparticles and their pharmacological applications: present status and application prospects. Springer, Berlin Heidelberg

Kim HN, Ren WX, Kim JS, Yoon J (2012) Fluorescent and colorimetric sensors for detection of lead{,} cadmium{,} and mercury ions. Chem Soc Rev 41:3210–3244. https://doi.org/10.1039/C1CS15245A

Kumar A, Hens A, Arun R, Mahato K, Chatterjee M, Layek K, Chanda N (2015) A paper based microfluidic device for easy detection of uric acid using positively charged gold nanoparticles. Analyst 140:1817–1820. https://doi.org/10.1039/C4AN02333A

Kumar N, Madhwal D, Jain VK, Suman (2020) A POC device for on-the-spot detection of hexavalent chromium in wastewater. J Environ Chem Eng 8:104342. https://doi.org/10.1016/j.jece.2020.104342

Kumari A, Singla R, Guliani A, Yadav SK (2014) Nanoencapsulation for drug delivery. EXCLI J 13:265–286

Lee J-S, Mirkin CA (2008) Chip-based Scanometric detection of mercuric ion using DNA-functionalized gold nanoparticles. Anal Chem 80:6805–6808. https://doi.org/10.1021/ac801046a

Li M, Gou H, Al-Ogaidi I, Wu N (2013) Nanostructured sensors for detection of heavy metals: a review. ACS Sustain Chem Eng 1:713–723. https://doi.org/10.1021/sc400019a

Li P, Wu Y, Li D, Su X, Luo C, Wang Y, Hu J, Li G, Jiang H, Zhang W (2018a) Seed-mediated synthesis of tunable-aspect-ratio gold Nanorods for near-infrared photoacoustic imaging. Nanoscale Res Lett 13:313. https://doi.org/10.1186/s11671-018-2734-8

Li S, Wei T, Tang M, Chai F, Qu F, Wang C (2018b) Facile synthesis of bimetallic ag-cu nanoparticles for colorimetric detection of mercury ion and catalysis. Sensors Actuators B Chem 255:1471–1481. https://doi.org/10.1016/j.snb.2017.08.159

Li X, Ballerini DR, Shen W (2012) A perspective on paper-based microfluidics: current status and future trends. Biomicrofluidics 6:11301. https://doi.org/10.1063/1.3687398

Li Y, Zaluzhna O, Xu B, Gao Y, Modest JM, Tong YJ (2011) Mechanistic insights into the Brust−Schiffrin two-phase synthesis of Organo-chalcogenate-protected metal nanoparticles. J Am Chem Soc 133:2092–2095. https://doi.org/10.1021/ja1105078

Liu J, Lu Y (2003) A colorimetric Lead biosensor using DNAzyme-directed assembly of gold nanoparticles. J Am Chem Soc 125:6642–6643. https://doi.org/10.1021/ja034775u

Liu JM, Wang HF, Yan XP (2011) A gold nanorod based colorimetric probe for the rapid and selective detection of Cu2+ ions. Analyst 136:3904–3910. https://doi.org/10.1039/c1an15460e

Liu L, Leng Y, Lin H (2016) Photometric and visual detection of Cr (VI) using gold nanoparticles modified with 1, 5-diphenylcarbazide. Microchimica Acta 183:1367–1373. https://doi.org/10.1007/s00604-016-1777-8

Liu Y, Wang X (2013) Colorimetric speciation of Cr(iii) and Cr(vi) with a gold nanoparticle probe. Anal Methods 5:1442–1448. https://doi.org/10.1039/c3ay00016h

Lo S, Wu M, Venkatesan P, Wu S (2015) Sensors and actuators B: chemical colorimetric detection of chromium (III) using O-phospho- l -serine dithiocarbamic acid functionalized gold nanoparticles. Sensors Actuators B Chem 220:772–778. https://doi.org/10.1016/j.snb.2015.05.120

Lu Y, Liang X, Niyungeko C, Zhou J, Xu J, Tian G (2018) A review of the identification and detection of heavy metal ions in the environment by voltammetry. Talanta 178:324–338. https://doi.org/10.1016/j.talanta.2017.08.033

Lussier F, Thibault V, Charron B, Wallace GQ, Masson J-F (2020) Deep learning and artificial intelligence methods for Raman and surface-enhanced Raman scattering. TrAC Trends Anal Chem 124:115796. https://doi.org/10.1016/j.trac.2019.115796

Ma Y, Niu H, Zhang X, Cai Y (2011) Colorimetric detection of copper ions in tap water during the synthesis of silver/dopamine nanoparticles. Chem Commun 47:12643–12645. https://doi.org/10.1039/C1CC15048K

Maghsoudi AS, Hassani S, Mirnia K, Abdollahi M (2021) Recent advances in nanotechnology-based biosensors development for detection of arsenic, lead, mercury, and cadmium. Int J Nanomedicine 16:803–832. https://doi.org/10.2147/IJN.S294417

Mahato K, Maurya PK, Chandra P (2018) Fundamentals and commercial aspects of nanobiosensors in point-of-care clinical diagnostics. 3 Biotech 8:1–14. https://doi.org/10.1007/s13205-018-1148-8

Mahato K, Nagpal S, Shah MA, Srivastava A, Maurya PK, Roy S, Jaiswal A, Singh R, Chandra P (2019) Gold nanoparticle surface engineering strategies and their applications in biomedicine and diagnostics. 3 Biotech 9:1–19. https://doi.org/10.1007/s13205-019-1577-z

Mahato K, Purohit B, Kumar A, Chandra P (2020) Paper-based biosensors for clinical and biomedical applications: emerging engineering concepts and challenges, 1st edn. Elsevier B. V, Amsterdam

Mahato K, Srivastava A, Chandra P (2017) Paper based diagnostics for personalized health care: emerging technologies and commercial aspects. Biosens Bioelectron 96:246–259. https://doi.org/10.1016/j.bios.2017.05.001

Mao X, Li Z-P, Tang Z-Y (2011) One pot synthesis of monodispersed L-glutathione stabilized gold nanoparticles for the detection of Pb2+ ions. Front Mater Sci 5:322–328. https://doi.org/10.1007/s11706-011-0118-4

Mathaweesansurn A, Vittayakorn N, Detsri E (2020) Highly sensitive and selective colorimetric sensor of mercury (II) based on layer-by-layer deposition of gold/silver bimetallic nanoparticles. Molecules 25:4443. https://doi.org/10.3390/molecules25194443

McQuaid HN, Muir MF, Taggart LE, McMahon SJ, Coulter JA, Hyland WB, Jain S, Butterworth KT, Schettino G, Prise KM, Hirst DG, Botchway SW, Currell FJ (2016) Imaging and radiation effects of gold nanoparticles in tumour cells. Sci Rep 2016:6. https://doi.org/10.1038/srep19442

Mehta VN, Kumar MA, Kailasa SK (2013) Colorimetric detection of copper in water samples using dopamine dithiocarbamate-functionalized au nanoparticles. Ind Eng Chem Res 52:4414–4420. https://doi.org/10.1021/ie302651f

Meng L, Zhang J, Li H, Zhao W, Zhao T (2019) Preparation and progress in application of gold Nanorods. J Nanomater 2019:1–11. https://doi.org/10.1155/2019/4925702

Moore TL, Rodriguez-Lorenzo L, Hirsch V, Balog S, Urban D, Jud C, Rothen-Rutishauser B, Lattuada M, Petri-Fink A (2015) Nanoparticle colloidal stability in cell culture media and impact on cellular interactions. Chem Soc Rev 44:6287–6305. https://doi.org/10.1039/C4CS00487F

Murphy CJ, Thompson LB, Chernak DJ, Yang JA, Sivapalan ST, Boulos SP, Huang J, Alkilany AM, Sisco PN (2011) Gold nanorod crystal growth: from seed-mediated synthesis to nanoscale sculpting. Curr Opin Colloid Interface Sci 16:128–134. https://doi.org/10.1016/j.cocis.2011.01.001

Murty BS, Shankar P, Raj B, Rath BB, Murday J (2013) Synthesis routes. In: Textbook of nanoscience and nanotechnology. Springer, Berlin Heidelberg, pp 66–106

Mutlu AY, Kiliç V, Özdemir GK, Bayram A, Horzum N, Solmaz ME (2017) Smartphone-based colorimetric detection: via machine learning. Analyst 142:2434–2441. https://doi.org/10.1039/c7an00741h

Narayanan K, Sakthivel N (2008) Coriander leaf mediated biosynthesis of gold nanoparticles. Mater Lett 62:4588–4590. https://doi.org/10.1016/j.matlet.2008.08.044

Nath P, Arun RK, Chanda N (2014) A paper based microfluidic device for the detection of arsenic using a gold nanosensor. RSC Adv 4:59558–59561. https://doi.org/10.1039/c4ra12946f

Nath P, Arun RK, Chanda N (2015) Smart gold nanosensor for easy sensing of lead and copper ions in solution and using paper strips. RSC Adv 6:69024–69031. https://doi.org/10.1039/c5ra14886c

Nath P, Priyadarshni N, Chanda N (2018a) Europium-coordinated gold nanoparticles on paper for the colorimetric detection of arsenic(III, V) in aqueous solution. ACS Appl Nano Mater 1:73–81. https://doi.org/10.1021/acsanm.7b00038

Nath P, Priyadarshni N, Mandal S, Singh P, Arun RK, Chanda N (2018b) Gold nanostructure in sensor technology: detection and estimation of chemical pollutants. In: Environmental, chemical and medical sensors. Springer, Singapore

Nghiem THL, La TH, Vu XH, Chu VH, Nguyen TH, Le QH, Fort E, Do QH, Tran HN (2010) Synthesis, capping and binding of colloidal gold nanoparticles to proteins. Adv Nat Sci Nanosci Nanotechnol 1:25009. https://doi.org/10.1088/2043-6254/1/2/025009

Nikoobakht B, El-Sayed MA (2003) Preparation and growth mechanism of gold Nanorods (NRs) using seed-mediated growth method. Chem Mater 15:1957–1962. https://doi.org/10.1021/cm020732l

Olenin AY (2019) Chemically modified silver and gold nanoparticles in spectrometric analysis. J. Anal. Chem 14:355–365

Pelin JNBD, Edwards-Gayle CJC, Martinho H, Gerbelli BB, Castelletto V, Hamley IW, Alves WA (2020) Self-assembled gold nanoparticles and amphiphile peptides: a colorimetric probe for copper(ii) ion detection. Dalt Trans 49:16226–16237. https://doi.org/10.1039/d0dt00844c

Perala SRK, Kumar S (2013) On the mechanism of metal nanoparticle synthesis in the Brust–Schiffrin method. Langmuir 29:9863–9873. https://doi.org/10.1021/la401604q

Placido T, Aragay G, Pons J, Comparelli R, Curri ML, Merkoçi A (2013) Ion-directed assembly of gold nanorods: a strategy for mercury detection. ACS Appl Mater Interfaces 5:1084–1092. https://doi.org/10.1021/am302870b

Polte J (2015) Fundamental growth principles of colloidal metal nanoparticles - a new perspective. CrystEngComm 2015:36. https://doi.org/10.1039/c5ce01014d

Poornima V, Alexandar V, Iswariya S, Perumal PT, Uma TS (2016) Gold nanoparticle-based nanosystems for the colorimetric detection of Hg2+ ion contamination in the environment. RSC Adv 6:46711–46722. https://doi.org/10.1039/c6ra04433f

Power AC, Morrin A (2013) Electroanalytical sensor technology. In: Khalid MAA (ed) Electrochemistry. IntechOpen, Rijeka

Prasad KS, Shruthi G, Shivamallu C (2018) Functionalized silver nano-sensor for colorimetric detection of Hg2+ ions: facile synthesis and docking studies. Sensors (Switzerland) 18:2698. https://doi.org/10.3390/s18082698

Priyadarshni N, Nath P, Nagahanumaiah CN (2018) DMSA-functionalized gold Nanorod on paper for colorimetric detection and estimation of arsenic (III and V) contamination in groundwater. ACS Sustain Chem Eng 6:6264–6272. https://doi.org/10.1021/acssuschemeng.8b00068

Rance GA, Marsh DH, Bourne SJ, Reade TJ, Khlobystov AN (2010) Van der Waals interactions between nanotubes and nanoparticles for controlled assembly of composite nanostructures. ACS Nano 4:4920–4928. https://doi.org/10.1021/nn101287u

Ratnarathorn N, Chailapakul O, Dungchai W (2015) Highly sensitive colorimetric detection of lead using maleic acid functionalized gold nanoparticles. Talanta 132:613–618. https://doi.org/10.1016/j.talanta.2014.10.024

Ravindran A, Elavarasi M, Prathna TC, Raichur AM, Chandrasekaran N, Mukherjee A (2012) Selective colorimetric detection of nanomolar Cr (VI) in aqueous solutions using unmodified silver nanoparticles. Sensors Actuators B Chem 166–167:365–371. https://doi.org/10.1016/j.snb.2012.02.073

Razzaque S, Hussain SZ, Hussain I, Tan B (2016) Design and utility of metal/metal oxide nanoparticles mediated by thioether end-functionalized polymeric ligands. Polymers (Basel) 8:156. https://doi.org/10.3390/polym8040156

Sackmann EK, Fulton AL, Beebe DJ (2014) The present and future role of microfluidics in biomedical research. Nature 507:181–189. https://doi.org/10.1038/nature13118

Saha K, Agasti SS, Kim C, Li X, Rotello VM (2012) Gold nanoparticles in chemical and biological sensing. Chem Rev 112:2739–2779. https://doi.org/10.1021/cr2001178

Sahin B, Kaya T (2019) Electrochemical amperometric biosensor applications of nanostructured metal oxides: a review. Mater Res Express 6:42003. https://doi.org/10.1088/2053-1591/aafa95

Sahu S, Sharma S, Ghosh KK (2020) Novel formation of au/ag bimetallic nanoparticles from a mixture of monometallic nanoparticles and their application for the rapid detection of lead in onion samples. New J Chem 44:15010–15017. https://doi.org/10.1039/D0NJ02994G

Sajed S, Arefi F, Kolahdouz M, Sadeghi MA (2019) Improving sensitivity of mercury detection using learning based smartphone colorimetry. Sensors Actuators B Chem 298:126942. https://doi.org/10.1016/j.snb.2019.126942

Sajed S, Kolahdouz M, Sadeghi MA, Razavi SF (2020) High-performance estimation of lead ion concentration using smartphone-based colorimetric analysis and a machine learning approach. ACS Omega 5:27675–27684. https://doi.org/10.1021/acsomega.0c04255

Salem SS, Fouda A (2021) Green synthesis of metallic nanoparticles and their prospective biotechnological applications: an overview. Biol Trace Elem Res 199:344–370. https://doi.org/10.1007/s12011-020-02138-3

Salimi F, Zarei K, Karami C (2018) Naked eye detection of Cr 3 + and Ni 2 + ions by gold nanoparticles modified with ribavirin. Silicon 10:1755–1761

Santos GA d (2017) The importance of metallic materials as biomaterials. Adv Tissue Eng Regen Med 3:1. https://doi.org/10.15406/atroa.2017.03.00054

Scozzari A (2008) Electrochemical sensing methods: a brief review andrea scozzari. Methods 5:335–351

Sengani M, Grumezescu AM, Rajeswari VD (2017) Recent trends and methodologies in gold nanoparticle synthesis – a prospective review on drug delivery aspect. OpenNano 2:37–46. https://doi.org/10.1016/j.onano.2017.07.001

Shellaiah M, Simon T, Venkatesan P, Sun KW, Ko F, Wu S (2018) Nanodiamonds conjugated to gold nanoparticles for colorimetric detection of clenbuterol and chromium (III) in urine. Microchimica Acta 185:1–8

Shrivas K, Patel S, Sinha D, Thakur S, Patle T, Kant T, Dewangan K, Satnami M, Nirmalkar J, Kumar S (2020) Colorimetric and smartphone-integrated paper device for on-site determination

of arsenic (III) using sucrose modified gold nanoparticles as a nanoprobe. Microchim Acta 187: 1–9. https://doi.org/10.1007/s00604-020-4129-7

Shrivas K, Sahu B, Deb MK, Thakur SS, Sahu S, Kurrey R, Kant T, Patle TK, Jangde R (2019) Colorimetric and paper-based detection of lead using PVA capped silver nanoparticles: experimental and theoretical approach. Microchem J 150:104156. https://doi.org/10.1016/j.microc.2019.104156

Shrivas K, Sahu S, Patra GK, Jaiswal NK, Shankar R (2016) Localized surface plasmon resonance of silver nanoparticles for sensitive colorimetric detection of chromium in surface water{,} industrial waste water and vegetable samples. Anal Methods 8:2088–2096. https://doi.org/10.1039/C5AY03120F

Shrivas K, Shankar R, Dewangan K (2015) Gold nanoparticles as a localized surface plasmon resonance based chemical sensor for on-site colorimetric detection of arsenic in water samples. Sensors Actuators B Chem 220:1376–1383. https://doi.org/10.1016/j.snb.2015.07.058

Singla R, Guliani A, Kumari A, Yadav SK (2016) Metallic nanoparticles, toxicity issues and applications in medicine. In: Yadav SK (ed) Nanoscale materials in targeted drug delivery, Theragnosis and tissue regeneration. Springer, Singapore, pp 41–80

Siontorou CG, Nikoleli G-P, Nikolelis M-T, Nikolelis DP (2019) Challenges and future prospects of Nanoadvanced sensing technology. Elsevier, Amsterdam

Sperling RA, Parak WJ (2010) Surface modification, functionalization and bioconjugation of colloidal inorganic nanoparticles. Philos. Trans. R. Soc. A Math. Phys. Eng. Sci 368:1333–1383

Su D, Yang X, Xia Q, Chai F, Wang C, Qu F (2013) Colorimetric detection of Hg2+ using thioctic acid functionalized gold nanoparticles. RSC Adv 3:24618–24624. https://doi.org/10.1039/C3RA43276A

Tchounwou PB, Yedjou CG, Patlolla AK, Sutton DJ (2012) Heavy metal toxicity and the environment. Exp Suppl 101:133–164

Turkevich J, Stevenson PC, Hillier J (1951) A study of the nucleation and growth processes in the synthesis of colloidal gold. Discuss Faraday Soc 11:55–75. https://doi.org/10.1039/DF9511100055

Varun S, Kiruba Daniel SCG (2018) Emerging nanosensing strategies for heavy metal detection. Nanotechnol Sustain Water Resour 5:199–225. https://doi.org/10.1002/9781119323655.ch7

Vasquez G, Hernández Y, Coello Y (2018) Portable low-cost instrumentation for monitoring Rayleigh scattering from chemical sensors based on metallic nanoparticles. Sci Rep 8:14903. https://doi.org/10.1038/s41598-018-33271-8

Venkatesh N (2018) Metallic nanoparticle: a review. Biomed J Sci Tech Res 4:3765–3775. https://doi.org/10.26717/bjstr.2018.04.0001011

Vigderman L, Khanal BP, Zubarev ER (2012) Functional gold Nanorods: synthesis, self-assembly, and sensing applications. Adv Mater 24:4811–4841. https://doi.org/10.1002/adma.201201690

Wang AJ, Guo H, Zhang M, Zhou DL, Wang RZ, Feng JJ (2013) Sensitive and selective colorimetric detection of cadmium (II) using gold nanoparticles modified with 4-amino-3-hydrazino-5-mercapto-1,2,4-triazole. Microchim Acta 180:1051–1057. https://doi.org/10.1007/s00604-013-1030-7

Wang C, Yu C (2013) Detection of chemical pollutants in water using gold nanoparticles as sensors: a review. Rev Anal Chem 32:1–14. https://doi.org/10.1515/revac-2012-0023

Wang H, Yang L, Chu S, Liu B, Zhang Q, Zou L, Yu S, Jiang C (2019) Semiquantitative visual detection of Lead ions with a smartphone via a colorimetric paper-based analytical device. Anal Chem 91:9292–9299. https://doi.org/10.1021/acs.analchem.9b02297

Wang X, Wei Y, Wang S, Chen L (2015) Colloids and surfaces a: physicochemical and engineering aspects red-to-blue colorimetric detection of chromium via Cr (III) -citrate chelating based on tween 20-stabilized gold nanoparticles. Colloids Surfaces A Physicochem Eng Asp 472:57–62. https://doi.org/10.1016/j.colsurfa.2015.02.033

Wang Y, Xia Y (2004) Bottom-up and top-down approaches to the synthesis of monodispersed spherical colloids of low melting-point metals. Nano Lett 4:2047–2050. https://doi.org/10.1021/nl048689j

Wang Y-W, Wang M, Wang L, Xu H, Tang S, Yang H-H, Zhang L, Song H (2017) A simple assay for ultrasensitive colorimetric detection of ag+ at Picomolar levels using platinum nanoparticles. Sensors 17:2521. https://doi.org/10.3390/s17112521

Willner MR, Vikesland PJ (2018) Nanomaterial enabled sensors for environmental contaminants prof Ueli Aebi, prof Peter Gehr. J Nanobiotechnology 16:1–16. https://doi.org/10.1186/s12951-018-0419-1

Wu Y, Zhan S, Wang F, He L, Zhi W, Zhou P (2012) Cationic polymers and aptamers mediated aggregation of gold nanoparticles for the colorimetric detection of arsenic(iii) in aqueous solution. Chem Commun 48:4459–4461. https://doi.org/10.1039/C2CC30384A

Xiong W, Ndokoye P, Leung MKH (2019) Noble metal-based nanosensors for environmental detection. Elsevier, Amsterdam

Xiong X, Zhang J, Wang Z, Liu C, Xiao W, Han J, Shi Q (2020) Simultaneous multiplexed detection of protein and metal ions by a colorimetric microfluidic paper-based analytical device. Biochip J 14:429–437. https://doi.org/10.1007/s13206-020-4407-9

Xu Y, Dong Y, Jiang X, Zhu N (2013) Colorimetric detection of trivalent chromium in aqueous solution using tartrate-capped silver nanoparticles as probe. J Nanosci Nanotechnol 13:6820–6825. https://doi.org/10.1166/jnn.2013.7785

Xue Y, Zhao H, Wu Z, Li X, He Y, Yuan Z (2011) Colorimetric detection of Cd2+ using gold nanoparticles cofunctionalized with 6-mercaptonicotinic acid and l-cysteine. Analyst 136:3725–3730. https://doi.org/10.1039/c1an15238f

Yasun E, Kang H, Erdal H, Cansiz S, Ocsoy I, Huang YF, Tan W (2013) Cancer cell sensing and therapy using affinity tag-conjugated gold nanorods. Interface Focus 3:1–9. https://doi.org/10.1098/rsfs.2013.0006

Ye Y, Lv M, Zhang X, Zhang Y (2015) Colorimetric determination of copper(ii) ions using gold nanoparticles as a probe. RSC Adv 5:102311–102317. https://doi.org/10.1039/c5ra20381c

Yeh Y-C, Creran B, Rotello VM (2012) Gold nanoparticles: preparation{,} properties{,} and applications in bionanotechnology. Nanoscale 4:1871–1880. https://doi.org/10.1039/C1NR11188D

Yetisen AK, Akram MS, Lowe CR (2013) Paper-based microfluidic point-of-care diagnostic devices. Lab Chip 13:2210–2251. https://doi.org/10.1039/C3LC50169H

Yu C-J, Tseng W-L (2008) Colorimetric detection of mercury(II) in a high-salinity solution using gold nanoparticles capped with 3-Mercaptopropionate acid and adenosine monophosphate. Langmuir 24:12717–12722. https://doi.org/10.1021/la802105b

Yu L, Li N (2019) Noble metal nanoparticles-based colorimetric biosensor for visual quantification: a mini review. Chemosensors 7:53. https://doi.org/10.3390/chemosensors7040053

Yu M (2014) Colorimetric detection of trace arsenic(III) in aqueous solution using arsenic aptamer and gold nanoparticles. Aust J Chem 67:813. https://doi.org/10.1071/CH13512

Zhang D, Ma X, Gu Y, Huang H, Zhang G (2020) Green synthesis of metallic nanoparticles and their potential applications to treat cancer. Front Chem 8:799. https://doi.org/10.3389/fchem.2020.00799

Zhang G (2013) Functional gold nanoparticles for sensing applications. Nanotechnol Rev 2:269–288. https://doi.org/10.1515/ntrev-2012-0088

Zhang J, Sun X, Wu J (2019a) Heavy metal ion detection platforms based on a glutathione probe: a mini review. Appl Sci 9:489. https://doi.org/10.3390/app9030489

Zhang J, Zhu K, Hao H, Huang G, Gan W, Wu K, Zhang Z, Fu X (2019b) A novel chitosan modified Au@Ag core-shell nanoparticles sensor for naked-eye detection of Hg2. Mater Res Express 6:125045. https://doi.org/10.1088/2053-1591/ab57b8

Zhang Z, Chen Z, Qu C, Chen L (2014) Highly sensitive visual detection of copper ions based on the shape-dependent LSPR spectroscopy of gold nanorods. Langmuir 30:3625–3630. https://doi.org/10.1021/la500106a

Zheng B, Li J, Zheng Z, Zhang C, Huang C, Hong J, Li Y, Wang J (2021) Rapid colorimetric detection of arsenic (III) by glutathione functionalized gold nanoparticles based on RGB

extracting system. Opt Laser Technol 133:106522. https://doi.org/10.1016/j.optlastec.2020.106522

Zhou J, Ralston J, Sedev R, Beattie DA (2009) Functionalized gold nanoparticles: synthesis, structure and colloid stability. J Colloid Interface Sci 331:251–262. https://doi.org/10.1016/j.jcis.2008.12.002

Zhou Y, Zhao H, He Y, Ding N, Cao Q (2011) Colorimetric detection of Cu2+ using 4-mercaptobenzoic acid modified silver nanoparticles. Colloids Surfaces A Physicochem Eng Asp 391:179–183. https://doi.org/10.1016/j.colsurfa.2011.07.026

Zhu J, Yu YQ, Li JJ, Zhao JW (2016) Colorimetric detection of lead(ii) ions based on accelerating surface etching of gold nanorods to nanospheres: the effect of sodium thiosulfate. RSC Adv 6:25611–25619. https://doi.org/10.1039/c5ra26560f

Zhu T, Vasilev K, Kreiter M, Mittler S, Knoll W (2003) Surface modification of citrate-reduced colloidal gold nanoparticles with 2-Mercaptosuccinic acid. Langmuir 19:9518–9525. https://doi.org/10.1021/la035157u